TITLE OF THE INVENTION

METHOD AND BIOMARKERS FOR DETECTING TUMOR ENDOTHELIAL CELL
PROLIFERATION

5   CROSS-REFERENCE TO RELATED APPLICATIONS

The present application claims the benefit U.S. Provisional Application No. 60/556,645, filed
March 26, 2004, hereby incorporated by reference herein.

FIELD OF THE INVENTION

10   The field of this invention relates to methods, biomarkers, and expression signatures for
assessing the proliferative rate of vascular endothelial cells within tumors. More specifically, the
invention provides a set of genes which can be used as biomarkers for evaluating the pharmacodynamic
effects of cancer therapies designed to regulate the proliferation of endothelial cells in tumor vasculature.
In one aspect the invention provides a method of evaluating the efficacy of a compounds designed to

15   inhibit kinase receptor activity, such as a mammalian KDR receptor activity.

BACKGROUND OF THE INVENTION

In the description that follows, the teachings of various scientific references are relied on to
support particular findings and statements. The numerical citations included at the end of particular
sentences refer to the numbered list of references included at the end of the specification.

20   Vascular endothelial cells form a luminal non-thrombogenic monolayer throughout the vascular
system. Solid tumors require a vascular system to expand beyond small nodules limited by the diffusion
of nutrients and metabolic by products. Although tumor cells can initially colonize existing host
capillaries, their growth leads to the collapse of these preexisting normal vessels resulting in hypoxia.

25   Therefore, angiogenesis is critical to the progression of numerous cancers. Subsequent tumor growth
requires neovascularization that is achieved by the ingrowth of new host blood vessels, denoted tumor
angiogenesis. Tumors induce proliferation, migration and differentiation resulting in neovascularization
by secreting growth factors for vascular endothelial cells. Angiogenesis is critical to the progression of
numerous cancers. Tumors induce endothelial cell migration, proliferation and differentiation resulting

30   in neovascularization arising from existing blood vessels. Tumor cells induce angiogenesis primarily
through the production and secretion of vascular endothelial growth factor (VEGF), a secreted protein
that is a potent endothelial cell mitogen and ligand for the kinase insert domain receptor (KDR, FLK-1,
or VEGF receptor).

Tyrosine kinases are a class of enzymes that catalyze the transfer of the terminal phosphate of

35   adenosine triphosphate to tyrosine residues in protein substrates. Tyrosine kinases are believed, by way

of substrate phosphorylation, to play critical roles in signal transduction for a number of cell functions and have been shown to be important contributing factors in cell proliferation, carcinogenesis and cell differentiation. Tyrosine kinases can be categorized as receptor type or non receptor type. Receptor type tyrosine kinases typically have an extracellular, a transmembrane, and an intracellular portion, while non-receptor type tyrosine kinases typically are wholly intracellular, while examples exist of membrane receptors that upon ligand binding recruit intracellular kinases to bind to the intracellular portion of the receptor which, by itself, does not have kinase activity. Both receptor-type and non-receptor type tyrosine kinases are implicated in cellular signaling pathways leading to numerous pathogenic conditions, including cancer, psoriasis and hyperimmune responses.

The receptor-type tyrosine kinases are comprised of a large number of transmembrane receptors with diverse biological activity. In fact, about twenty different subfamilies of receptor-type tyrosine kinases have been identified. The kinase insert domain receptor (KDR) belongs to the FLK subfamily of receptor-type tyrosine kinases. KDR is a transmembrane receptor tyrosine kinase expressed primarily in vascular endothelial cells that transduces the majority of physiological functions attributed to VEGF (3, 8-10). Inhibition of KDR catalytic activity blocks tumor neo-angiogenesis, reduces vascular permeability, and, in animal models, inhibits tumor growth and metastasis.

Tumor cells induce angiogenesis primarily through the production and secretion of vascular endothelial growth factor (VEGF) a potent endothelial cell mitogen and ligand for the kinase insert domain receptor (KDR, FLK-1, or VEGF receptor 2) (3-7). VEGF binds with high affinity to two transmembrane tyrosine kinase-linked receptors, Flt-1 (VEGFR-1) and KDR (Flk-1/VEGFR-2), that are expressed by vascular endothelial cells. The binding of dimeric VEGF to the extracellular region of KDR promotes receptor dimerization that brings the intracellular tyrosine kinase domains together and promotes phosphorylation of several receptor tyrosine residues, at least some of which are critical for mitogenic signal transduction.

Extensive efforts are underway to identify anti-angiogenic therapies for the treatment of human cancers. Since VEGF produced and secreted by tumor cells activates KDR and induces endothelial cell proliferation, inhibition of KDR by a small molecule should lead to a decrease in the proliferation rate of tumor endothelial cells. Currently, several small molecule inhibitors of KDR activity are being evaluated as anti-cancer agents in clinical trials. Once activated, KDR initiates a signal transduction cascade, is internalized and ultimately degraded. Inhibition of the VEGF/KDR system has been shown to inhibit VEGF-dependent tumor angiogenesis and growth in several animal models. Because VEGF produced and secreted by tumor cells activates KDR and induces endothelial cell proliferation, it is acknowledged that inhibition of KDR kinase activity should lead to decreases in the proliferation of tumor endothelial cells. Accordingly, numerous proposed cancer therapeutics target vascular endothelial cell growth factor

(VEGF) or the kinase insert domain receptor (KDR/VEGFR-2/FLK-1), the primary VEGF receptor on endothelial cells.

       Clinically, it is difficult to assess directly the pharmacodynamic effects of KDR inhibitors because KDR protein is not easily detectable in readily available clinical samples. Measurement of

5   changes in vascular permeability within a tumor by dynamic contrast-enhanced magnetic resonance imaging (DCE-MRI) is currently the most common pharmacodynamic assay, but provides an indirect readout and is a complex and expensive procedure. Thus, there is a need in the clinical setting for a rapid, quantitative, reproducible, and inexpensive assay that is compatible with current clinical laboratory instrumentation and which is capable of assessing the efficacy of anti-angiogenic agents.

10

SUMMARY OF THE INVENTION

       As the mitogenically and angiogenically competent VEGF receptor, KDR is a particularly attractive target to antagonize VEGF-dependent tumor angiogenesis and growth. Inhibition of KDR catalytic activity blocks tumor neoangiogenesis, reduces vascular permeability, and in animal moldes,

15   inhibits tumor growth and metastasis. However, because KDR protein is not expressed at high levels in readily accessible biological material, such as peripheral blood or bone marrow aspirates, clinical assessment of the *in vivo* pharmacodynamic efficacy of KDR kinase inhibitors is challenging. Accordingly, current pharmacodynamic assays for KDR inhibition generally rely on surrogate protein kinase markers whose activity is also sensitive to the compound being evaluated (i.e. Fms-related

20   tyrosine kinase-3 (Flt-3) tyrosine phosphorylation in the case of many KDR kinase inhibitors) or on imaging techniques such as DCE-MRI that can assess changes in vascular permeability. These methods have the disadvantage of being indirect measures of KDR function and endothelial cell proliferation.

       An alternate approach is to assess the pharmacodynamic effects of putative KDR inhibitors on the proliferation rate of tumor endothelial cells. One described method for the *in vivo* assessment of EC

25   proliferation involves dual immunohistochemical (IHC) staining of tumor sections for the endothelial cell marker CD-31 and a nuclear marker of cellular proliferation, Ki-67(11). While an immunohistochemical method such as this can determine the fraction of ECs that are proliferating, the experimental protocol is technically complex and difficult and the analysis required for each stained tumor section is extremely time-consuming. Each of these factors makes clinical use of an IHC-based assay unlikely.

30   The methods disclosed and claimed herein are based on the discovery and characterization of biomarkers and gene expression signatures that are specific for proliferating endothelial cells. Gene expression profiling data from cultured primary endothelial cells, cultured tumor cells, and tissue from animal tumor models treated with KDR inhbitors was used to identify a set of genes that are selectively overexpressed in tumor endothelial cells relative to tumor cells, and whose pattern of expression

35   correlates with the rate of tumor endothelial cell proliferation. It is contemplated that the biomarkers and

endothelial cell-specific expression signatures which are disclosed and claimed herein will find utility in the context of providing a pharmacodynamic readout for any cancer therapy that aims to inhibit proliferation of endothelial cells in tumor vasculature.

As shown herein, the expression levels of these genes serve as the basis of a simple

5   pharmacodynamic assay for the activity of small molecule inhibitors of the KDR receptor tyrosine kinase. The methods disclosed and claimed herein can be used as the basis for a pharmacodynamic assay capable of supporting the clinical development of small molecule inhibitors of the KDR receptor tyrosine kinase. More specifically, the invention provides a method for assessing the *in vivo* effects of a KDR kinase inhibitor on the proliferative rate of vascular endothelial cells within tumors.

10   In one aspect the invention provides a method for determining the proliferative status (or rate) of endothelial cells. As shown herein, the disclosed method can be used to evaluate the proliferative status of endothelial cells in either an *in vitro* or *in vivo* format. One of skill in the art will acknowledge that the disclosed gene expression-based pharmacodynamic assays which can be established based on the disclosure provided herein can be used to support screening assays established to evaluate the efficacy of

15   therapeutic agents intended to regulate the proliferative status of endothelial cells.

In a second aspect the invention provides a method for evaluating the proliferative rate of vascular endothelial cells within tumors. In a particular embodiment, the invention provides a gene expression-based pharmacodynamic assay that is suitable for use to support clinical development of cancer therapies designed to regulate the proliferation of endothelial cells in tumor vasculature. For

20   example, it is contemplated that the disclosed methods can be used to establish pharmacodynamic assays that can distinguish tumors containing proliferating endothelial cells from tumors containing mostly quiescent endothelial cells. In a particular embodiment the method may include detecting the expression level of one or more genes selected from a group consisting of Angpt-2, Clu (ApoJ), Cyr61 (CCN1), Endrb (Etb), Ifit-3 (Garg49), Fut-4, Plau (uPA).

25   In a third aspect the invention provides a method for evaluating the activity of anti-angiogenesis therapeutics intended to regulate the proliferative rate of vascular endothelial cells within tumors. In a particular embodiment, the invention provides a method for evaluating the efficacy of small molecule inhibitors of receptor-type kinase inhibitors, such as KDR. For example, this aspect of the invention provides a method which is suitable for use to support clinical development of KDR kinase inhibitors,

30   such as Compound A. Using the information provided herein, particularly the Compound A-and B-induced endothelial cell-specific expression signatures provided in Tables 5. Table 6 provides the summary information describing the changed (suppressed) expression of endothelial cell specific biomarkers (collectively referred to as the proliferation sequence) observed in response to the *in vivo* administration of KDR Kinase inhibitors (Compounds A and B), provided in Table 6. It is well within

- 4 -

the abilities of a skilled artisan to design and validate a gene expression-based assay that is suitable for evaluating the efficacy of anti-angiogenesis agents.

It is contemplated that using the disclosure provided herein a skilled artisan can utilize the information provided in the tables summarizing the proliferation signatures disclosed herein to identify

5   compound-specific expression signatures that will facilitate evaluating the efficacy of alternative therapeutic agents intended to regulate endothelial cell proliferation. For example, this aspect of the invention provides a method which is suitable for use to support clinical development of KDR kinase inhibitors, such as Compound A. For example, it is contemplated that the efficacy of Compound A could be evaluated *in vivo* by establishing an assay which detects changes in the expression of a gene signature

10   comprising the Angpt-2, Clu (ApoJ), Cyr61 (CCN1), Endrb (Etb), Ifit-3 (Garg49), Fut-4, Plau (uPA) genes.

In a fourth aspect, the invention provides a composition of genes or biomarkers which are selectively overexpressed in tumor endothelial cells relative to tumor cells, and whose pattern of expression correlates with the rate of tumor endothelial cell proliferation. One embodiment of this aspect

15   of the invention provides compositions comprising at least two oligonucleotides, wherein each of the oligonucleotides comprises a sequence that specifically hybridizes to a gene disclosed in Tables 3 or 4 as well as solid supports comprising at least two probes, wherein each of the probes comprises a sequence that specifically hybridizes to a gene in Tables 3, 4, 5 or 6. In a particular embodiment, the composition will comprise oligonucleotides and/or probes which hybridize with the following genes: Angpt-2, Clu

20   (ApoJ), Cyr61 (CCN1), Endrb (Etb), Ifit-3 (Garg49), Fut-4, Plau (uPA), in combination with other oligonucleotides or probes specific for other genes identified in Tables 3-6.

In another aspect the invention provides gene expression signatures, which can be used to establish expression-based pharmacodynamic assays for evaluating the efficacy of therapeutic agents designed to regulate the proliferation of endothelial cells. It is contemplated that one of skill in the art

25   will be able to utilize the information provided in this disclosure, in particular the information contained in the Proliferation Signature Tables, referred to herein as Table 3 (HDMVEC Proliferation Signature), Table 4 (RHMVEC Prolilferation Signature), Table 5 (Compound A-and B-induced Endothelial Cell Specific Sequences) and Table 6 (Changes in EC-specific proliferation signature by KDR Kinase Inhibitor Asministration), to elucidate endothelial cell proliferation signatures that are suitable for

30   monintoring the in efficacy of other anti-angiogenic compounds. As shown herein, the gene expression signature disclosed and claimed herein can be used distinguish tumors containing mostly proliferating ECs from tumors containing mostly quiescent ECs.

It is contemplated that the disclosed assay will have the ability to detect inhibition of angiogenesis relatively quickly after initiating therapy, eliminating the longer period of time required to

35   visualize morphological changes in tumor microvasculature. In addition, it is envisioned that the

disclosed methods will be particularly useful in circumstances where immunohistochemistry is inappropriate or impractical, such as with small tissue samples from biopsies (i.e. fine needle aspirates) or from tissue samples with poor morphology. In a real time quantitative reverse transcription-polymerase chain reaction (PCR) format, the disclosed assay is predicted to represent an extremely

5   sensitive assay that is readily compatible with existing clinical laboratory instrumentation.

Expression profiling-based monitoring of the pharmacodynamic effects of cancer therapy potentially has many benefits. Used in the clinical setting, this technology provides for rapid, quantitative, reproducible, and inexpensive assays that are compatible with current clinical laboratory instrumentation. Carefully designed, gene expression-based asssays, such as the assays disclosed herein,

10   have the potential to make dosing of anti-neoplastic agents more efficient, to identify patient populations most likely to benefit from specific therapies, and to reduce clinical development time of novel therapeutics. Each of these aspects will lead to increased tumor response rates and improved human health.

15   BRIEF DESCRIPTION OF THE DRAWINGS

Figures 1A and 1B. Inhibition of Vascular Endothelial Cell (VEC) proliferation *in vitro* by KDR kinase inhibition. HDMVECs or RHMVECs were trypsinization following the third passage in culture and seeded in fibronectin-coated, six-well tissue culture plates at a density of 10,000 cells/well. Cell growth was arrested for 24h by mitogen withdrawal and then stimulated by the addition of 100 ng/ml

20   VEGF, 100 ng/ml bFGF or 200 μg/ml ENDOGRO. Wells with unstimulated cells and wells containing un-arrested cells were included as controls. At 72 hr following growth factor stimulation, cells were removed from the culture plates by trypsinization and counted on a hemocytometer under bright-field microscopy.

Figures 2A and 2B. Identification of a gene expression profile in proliferating vascular

25   endothelial cells *in vitro*. HDMVECs and RHMVECs were grown in culture and mitogen deprived for 24 hr as described in Figure 1 and Methods. Following a 24 hr stimulation with growth factor, culture media was aspirated quickly and the cells lysed in an RNA stabilizing buffer. Matched control plates that received no supplemental stimulatory growth factor were present for each stimulation condition and RNAs isolated from them served as the reference to which the RNAs from the stimulated cells was

30   compared. Bars corresponding to genes which are regulated (e.g., upregulated or downregulated) are indicated by various shades of gray. Color intensity represents the degree of regulation, not mRNA copy number.

Figures 3A-3D. Specific suppression of VEGF-induced gene expression in cultured vascular endothelial cells. EC monolayers were maintained in complete MCDB-131 media until reaching ~75%

35   confluence, then induced into a quiescent state by mitogen starvation for 24 hr. Cells were then

stimulated to proliferate with 100 ng/ml VEGF for 24 hr in the presence or absence of Compound B. RNA populations isolated from cells exposed to VEGF or VEGF + Compound B were compared to matched control RNAs isolated from quiescent cells exposed to neither VEGF nor Compound B. Each point in the plots represents a gene sequence present on the DNA oligonucleotide microarray and is

5   plotted according to the ratio of the two mRNA levels (experimental sample intensity: control sample intensity, vertical-axis) and the total mRNA quantity (experimental sample intensity + control sample intensity, horizontal-axis) for that gene. Dark-colored points indicate upregulated genes. Light Gray colored points indicate downregulated genes.

       Figures 4A and 4B. Growth kinetics of established rat tumors following exposure to a KDR

10   kinase inhibitor. Tumor studies were performed as described in Materials and Methods. Figures 4A and 4B illustrate tumor volumes from animals in the C6 profiling study (Fig. 4A) and the MattIII profiling study (Fig. 4B) as determined by caliper measurements. Tumors were calipered in two dimensions (length and width) and tumor volume was calculated according to the formula (length) x (width) x (½ width).

15   Figures 5A-5C. Identification of gene expression changes induced in rat tumors by KDR kinase inhibitors *in vivo.*Each row represents a distinct tumor from an individual animal. Each column represents a gene. Gray colored points/bars indicate genes that are regulated (e.g., upregulated or downregulated) by KDR kinase. Figure 5A illustrates changes in the expression of genes from rat C6 flank tumors that are regulated following 24, 48, or 72 hrs of systemic exposure to the KDR kinase

20   inhibitor Compound B. Figure 5B illustrates changes in the expression of genes from rat C6 flank tumors regulated following 24, 48, or 72 hrs of systemic exposure to the KDR kinase inhibitor Compound A. Figure 5C illustrates changes in the expression of genes from rat MatBIII mammary tumors regulated following 100 hrs of systemic exposure to the KDR kinase inhibitor Compound A.

       Figures 6A-6B. Distinct tumor gene expression responses elicited by KDR inhibitors.TheVenn

25   diagram illustrated in figure 6A illustrates the degree of overlap between the tumor gene expression responses to KDR kinase inhibitors in C6 flank tumors and MatBIII mammary tumors. The Venn diagram provided in Panel B illustrates the degree of overlap between the sets of endothelial cell-specific genes regulated both *in vitro* by mitogens and in tumor tissue by KDR kinase inhibitors. All of the genes (biomakers) depicted in figure 6B are regulated *in vivo* by KDR kinase inhibitors in a manner opposite

30   that observed *in vitro* following exposure to mitogens.

       Figures 7A-7B. Confirmation of microarray data by real time quantitative real time PCR. Quantitative real time PCR was performed with gene-specific PCR primer pairs and amplicon-specific fluorescent probes (TaqMan). For each RNA sample tested, transcript abundance of GAPDH was determined. In addition, transcript abundance of genes of interest and GAPDH were determined for a

35   calibrator RNA sample (total rat lung RNA). Figure 7A illustrates fold changes in gene expression in

tumors from KDR kinase-treated animals relative tumors from vehicle-treated animals were calculated using the $\Delta\Delta CT$ method (see Materials and Methods). Figure 7B illustrates mRNA levels for each gene in the rat tumors relative the calibrator RNA pool.

Figure 8. Biomarker protein expression in rat mammary tumors is localized to vasculature. De-
5 waxed, re-hydrated MatBIII tumor sections were incubated with antibodies against CD31 and one of the following biomarker proteins: CLU, ANGPT2, CYR61, ENDRB, or PLAU. Primary antibodies bound to the biomarker proteins and CD31 were visualized with Alexa488-labeled and Alexa546-labeled secondary antibodies, respectively as described in Materials and Methods. After mounting under coverslips, images were captured with a Zeiss Axiocam through a Zeiss Axiovert 135 fluorescence
10 microscope equipped with a 40x objective and an Axiocam mHR CCD camera.

DETAILED DESCRIPTION OF THE INVENTION

In the description that follows, numerous terms and phrases known to those skilled in the art are used. In the interest of clarity and consistency of interpretation, the definitions of certain terms and
15 phrases are provided.

The present invention provides compositions and methods to detect the level of expression of genes that may be differentially expressed dependent upon the state of the cell, i.e., proliferating versus quiescent cells. As used herein, the phrase "detecting the level expression" includes methods that quantify expression levels as well as methods that determine whether a gene of interest is expressed at
20 all. Thus, an assay which provides a yes or no result without necessarily providing quantification of an amount of expression is an assay that requires "detecting the level of expression" as that phrase is used herein. The genes identified as being differentially expressed in proliferating endothelial cells may be used in a variety of nucleic acid detection assays to detect or quantify the expression level of a gene or multiple genes in a given sample. For example, traditional Northern blotting, nuclease protection, RT-
25 PCR and differential display methods may be used for detecting gene expression levels.

As used herein, oligonucleotide sequences that are complementary to one or more of the genes described herein, refers to oligonucleotides that are capable of hybridizing under stringent conditions to at least part of the nucleotide sequence of said genes. Such hybridizable oligonucleotides will typically exhibit at least about 75% sequence identity at the nucleotide level to said genes, preferably about 80%
30 or 85% sequence identity or more preferably about 90% or 95% or more sequence identity to said genes.

"Bind(s) substantially" refers to complementary hybridization between a probe nucleic acid and a target nucleic acid and embraces minor mismatches that can be accommodated by reducing the stringency of the hybridization media to achieve the desired detection of the target polynucleotide sequence.

The phrase "hybridizing specifically to" refers to the binding, duplexing or hybridizing of a molecule substantially to or only to a particular nucleotide sequence or sequences under stringent conditions when that sequence is present in a complex mixture (e.g., total cellular) DNA or RNA.

Assays and methods of the invention may utilize available formats to simultaneously screen at least about 100, preferably about 1000, more preferably about 10,000 and most preferably about 1,000,000 or more different nucleic acid hybridizations.

Directly assessing the pharmacodynamics of anti-angiogenesis therapeutics targeted to the VEGF signaling pathway is difficult. Inhibition of the KDR tyrosine protein kinase suppresses endothelial cell proliferation, but it is difficult to assess the rate of proliferation of these cells *in vivo*. One method that has been used is double immunohistochemical staining of tumor sections for CD31 and Ki67 in order to quantitate proliferating endothelial cells. A second method in use is to assess changes in vascular permeability by magnetic resonance imaging (MRI). Both methods have disadvantages. Immuno-histochemistry (IHC) is limited to studies where relatively large, intact tumor samples are available. Even then, it is rare to have paired tumor samples taken obtained before and after treatment with a drug candidate for comparison. Fine needle aspiration (FNA) biopsy samples from a clinical setting are not analyzable by this method. Furthermore, to accurately assess microvascular density or the percentage of proliferating endothelial cells throughout the tumor is labor intensive even with semi-automated or automated microscopy equipment. Analyzing MRI images to assess changes in vascular permeability is also labor intensive, requiring highly trained personnel both to operate the imager and to interpret the images.

Our strategy in designing a gene expression-based pharmacodynamic assay for endothelial cell proliferation was to employ genome-wide gene expression profiling to first identify a general mitogen-induced proliferation signature in cultured primary microvascular endothelial cells. Expression profiles of genes in particular, tissues, disease states or disease progression stages provide molecular tools for evaluating toxicity, drug efficacy, drug metabolism, development, and disease monitoring. Changes in the expression profile from a baseline profile can be used as an indication of such effects. Those skilled in the art can use any of a variety of known techniques to evaluate the expression of one or more of the genes and/or ESTs identified in the instant application in order to observe changes in the expression profile.

Beginning with a large set of genes shown to be regulated *in vitro* by mitogen-induced proliferation of primary endothelial cells, we identified a subset that was relatively specific to endothelial cells. We then identified the subset of genes from the *in vitro* proliferation signature that were endothelial cell-specific. Two distinct syngeneic tumor models are used to demonstrate that *in vivo* exposure to KDR kinase inhibitors mediated robust gene expression changes in a manner consistent with suppression of the proliferative rate of vascular endothelial cells within tumors. Gene expression

changes consistent with inhibition of VEGF-signaling and inhibition of endothelial cell proliferation were detected in tumors from each animal model.

The endothelial cell specificity of the putative biomarkers was confirmed by immuno-fluorescence microscopy. The biomakers were further validated by correlating their *in vivo* gene expression changes to an independent, immunohistochemical measure of endothelial cell proliferation.

Genes regulated by systemic exposure to KDR kinase inhibitors in at least two of the three tumor models were selected as endothelial cell proliferation biomarkers. Gene expression changes of these biomarkers (as determined by microarray hybridization) were confirmed by quantitative real time PCR, both in the tumors that were profiled as well as in tumors from an additional, independent animal tumor study.

The disclosed set of biomarkers was validated by correlating the compound-induced gene expression changes to compound-induced differences in proliferating tumor endothelial cell number as determined by immunohistochemical staining (again in the same rat tumors that were profiled). The endothelial cell specificity (in the context of our rat tumor models) of the biomarker expression (gene signature) disclosed and claimed herein expression is established by showing that the protein products of the identified genes are restricted to CD31-expressing cells. Based on the disclosure provided herein it is contemplated that it may be possible to identify a gene expression signature that reflects the proliferation rate of vascular endothelial cells within tumors, thereby allowing a clinician to predict tumor responsiveness to therapy.

Based on the data described herein, the instant invention provides a set of genes or biomarkers, collectively referred to herein as a gene signature, that are regulated both *in vitro* during mitogen-induced proliferation of primary microvascular endothelial cells and *in vivo* in response to systemic exposure to KDR kinase inhibitors. Changes in expression levels of these biomarkers in response to inhibition of KDR are indicators of change in tumor endothelial cell proliferation rate. It is contemplated that identification of the gene expression signature (or biomarkers) disclosed and claimed herein, the regulation of which indicative of changes in the proliferation rate of tumor vascular endothelial cells provides a non-invasive and inexpensive assay following exposure to anti-angiogenesis therapeutics.

While the expectation by random chance of identifying a gene that met all our selection criteria was low, we identified a set of seven potential biomarker genes (Angpt-2, Endrb (Etb), Fut-4, Clu (ApoJ), Cyr61 (CCN1), Plau (uPA), and Ifit-3 (Garg49)). Significantly, each of the seven identified biomarker is known or implicated to be involved in endothelial cell biology. We biased our biomarker selection towards endothelial cell specific genes, but there was no guarantee that genes meeting our multiple criteria would have any known function in endothelial cells. Surprisingly, nearly all the genes identified have been implicated or shown to be directly involved in the regulation of endothelial cell function.

The angiopoietin-2 protein (ANGPT2/ANG2) is a well characterized ligand for the Tie-2 receptor tyrosine kinase that functions in concert with VEGF and angiopoietin-1 to regulate vascular remodeling (25). Angiopoietin-2 gene expression has been previously reported to be directly upregulated by VEGF, both *in vivo* and *in vitro*, consistent with our results (26).

5   The type B endothelin receptor (EDNRB/ET(B)) is a seven transmembrane G-protein coupled receptor that is mutated in Waardenburg-Hirschsprung disease, a congenital malformation of neuronal ganglia in the hindgut (27). Most published studies of EDNRB describe its role in the neuronal system during neural crest development. However, it does control vasoconstriction and vascular cell proliferation induced by the endothelins and EDNRB has been shown to be overexpressed in primary

10   melanomas(28). EDNRB antagonists have been reported to inhibit vascular cell proliferation and human melanoma cell growth *in vitro* and *in vivo* (29, 30).

Fucosyltransferase 4 (FUT4) is an alpha1, 3-fucosyltransferase involved in the synthesis of myeloglycan, the major physiological binder of E-selectin (31). It is also involved in the synthesis of many other glycosylated proteins, but it is reported to be highly expressed in some tumors with inverse

15   correlation to prognosis (32).

Clusterin is a secreted glycoprotein that appears to be overexpressed in apoptotic cells (33-35) but whose function is still largely unknown (33). Clusterin expression has been shown to be anti-proliferative (36) and down-regulated in advanced prostate cancer (37-39). Reduction in serum clusterin levels also correlates with esophageal squamous cell carcinoma tumorigenesis (40).

20   Cysteine rich protein 61 (CYR61) is an extracellular matrix-associated heparin-binding protein with pro-angiogenic properties (41). *In vitro* CYR61, promotes cell adhesion to extracellular matrix and chemotaxis (42, 43). It stimulates cell motility through interaction with integrin $\alpha V\beta5$, $\alpha6\beta1$, $\alpha M\beta2$ and stimulates endothelial cell proliferation through interaction with aVb3 (44-48). Our observations that the Cyr61 gene was upregulated in rat tumor tissue following exposure to KDR kinase inhibitors did not

25   appear to be in agreement with an inhibition of endothelial cell proliferation. However it may be that the upregulation of the Cyr61 gene is a response mechanism the endothelial cell attempting to compensate for the lack of functional KDR.

The urokinase type-plasminogen activator (PLAU or uPA) is a proteolytic enzyme that plays a critical role in angiogenesis, tumor invasion, and metastasis by contributing to remodeling of the

30   extracellular matrix (49, 50). It has been characterized as a pro-tumor invasion and pro-metastatic factor. The effect of PLAU activity is the conversion of plasminogen to plasmin. As with Cyr61, it is unclear why we observe an increase in Plau gene expression in tumors exposed to KDR kinase inhibitors rather than the decrease we would have expected to accompany a decrease in neovascularization. We can surmise that increased Plau expression is a compensatory mechanism elicited by inhibition of the VEGF

signaling pathway, but clearly, more investigation is required to determine the mechanism underlying our observations.

Ifit3 (interferon-induced protein with tetratricopeptide repeats 3, also known as Garg-49 (glucocorticoid-attenuated response genes) and IRG2 (interferon responsive gene 2) is a gene that as yet

5   has no known function. Cloned from the mouse as part of studies to identify glucocorticoid attenuated response genes induced by lipopolysaccharide or interferon, the highly conserved tetratricopeptide repeat domains of IFIT3 are believed to mediate protein-protein interactions (51-54). No human ortholog of Ifit3 has been identified in human cells, but a homologous gene designated Ift4 is 60% identical and 78% similar by protein sequence (BLASTP, (55))

10   In practice a gene expression-based pharmacodynamic assay based on a small number of genes can be performed with relatively little effort using existing quantitative real time PCR technology familiar to clinical laboratories. Sufficient RNA for real time PCR can be isolated from low milligram quantities of sample tissue. Quantitative thermal cyclers may now be used with microfluidics cards pre-loaded with reagents making routine clinical use of multigene expression-based assays a realistic goal.

15   It is to be understood that alternative assay formats, other than the methodologies exemplified herein, may be used to monitor the ability of putative cancer therapeutic agent to modulate the expression of a gene identified in Tables 3-6. For instance, as described above, mRNA expression may be monitored directly by hybridization of probes to the nucleic acids of the invention. However, methods and assays of the invention are most efficiently designed with array or chip hybridization-based methods

20   for detecting the expression of a large number of genes. Any hybridization assay format may be used, including solution-based and solid support-based assay formats. A preferred solid support is a high density array also known as a DNA chip or a gene chip. In one assay format, gene chips containing probes to at least two genes from Tables 5-6 may be used to directly monitor or detect changes in gene expression in biological samples containing endothelial cells prepared from subjects exposed to putative

25   cancer therapeutics designed to regulate the proliferation of endothelial cells in tumor vasculature.

Solid supports containing oligonucleotide probes for differentially expressed genes can be any solid or semisolid support material known to those skilled in the art. Suitable examples include, but are not limited to, membranes, filters, tissue culture dishes, polyvinyl chloride dishes, beads, test strips, silicon or glass based chips and the like. Suitable glass wafers and hybridization methods are widely

30   available, for example, those disclosed by Beattie (WO 95/11755). Any solid surface to which oligonucleotides can be bound, either directly or indirectly, either covalently or non-covalently, can be used. In some embodiments, it may be desirable to attach some oligonucleotides covalently and others non-covalently to the same solid support.

A preferred solid support is a high density array or DNA chip. These contain a particular

35   oligonucleotide probe in a predetermined location on the array. Each predetermined location may contain

more than one molecule of the probe, but each molecule within the predetermined location has an identical sequence. Such predetermined locations are termed features. There may be, for example, from 2, 10, 100, 1000 to 10,000, 100,000 or 400,000 of such features on a single solid support. The solid support, or the area within which the probes are attached may be on the order of a square centimeter.

5   Oligonucleotide probe arrays for expression monitoring can be made and used according to any techniques known in the art (see for example, Lockhart et al., Nat. Biotechnol. (1996) 14, 1675-1680; McGall et al., Proc. Nat. Acad. Sci. USA (1996) 93, 13555-13460). Such probe arrays may contain at least two or more oligonucleotides that are complementary to or hybridize to two or more of the genes described herein. Such arrays my also contain oligonucleotides that are complementary or hybridize to at

10   least 3, 4, 5, 6, 7, 8, 9, 10, 20, 30, 50, 70 or more the genes described herein.

Any hybridization assay format may be used, including solution-based and solid support-based assay formats. Solid supports containing oligonucleotide probes for differentially expressed genes of the invention can be filters, polyvinyl chloride dishes, silicon or glass based chips, etc. Such wafers and hybridization methods are widely available, for example, those disclosed by Beattie (WO 95/11755). Any

15   solid surface to which oligonucleotides can be bound, either directly or indirectly, either covalently or non-covalently, can be used. A preferred solid support is a high density array or DNA chip. These contain a particular oligonucleotide probe in a predetermined location on the array. Each predetermined location may contain more than one molecule of the probe, but each molecule within the predetermined location has an identical sequence. Such predetermined locations are termed features. There may be, for

20   example, about 2, 10, 100, 1000 to 10,000; 100,000 or 400,000 of such features on a single solid support. The solid support, or the area within which the probes are attached may be on the order of a square centimeter.

Of the techniques listed above, the most sensitive and most flexible, quantitative method is RT-PCR, which can be used to compare mRNA levels in different sample populations, in normal and tumor

25   tissues, with or without drug treatment, to characterize patterns of gene expression, to discriminate between closely related mRNAs, and to analyze RNA structure.

The first step is the isolation of mRNA from a target sample. The starting material is typically total RNA isolated from human tumors or tumor cell lines, and corresponding normal tissues or cell lines, respectively. Thus RNA can be isolated from a variety of primary tumors, including breast, lung,

30   colon, prostate, brain, liver, kidney, pancreas, spleen, thymus, testis, ovary, uterus, etc., tumor, or tumor cell lines, with pooled DNA from healthy donors. If the source of mRNA is a primary tumor, mRNA can be extracted, for example, from frozen or archived paraffin-embedded and fixed (e.g. formalin-fixed) tissue samples.

As RNA cannot serve as a template for PCR, the first step in gene expression profiling by RT-

35   PCR is the reverse transcription of the RNA template into cDNA, followed by its exponential

amplification in a PCR reaction. The two most commonly used reverse transcriptases are avilo myeloblastosis virus reverse transcriptase (AMV-RT) and Moloney murine leukemia virus reverse transcriptase (MMLV-RT). The reverse transcription step is typically primed using specific primers, random hexamers, or oligo-dT primers, depending on the circumstances and the goal of expression

5   profiling. For example, extracted RNA can be reverse-transcribed using a GeneAmp RNA PCR kit (Perkin Elmer, California, USA), following the manufacturer's instructions. The derived cDNA can then be used as a template in the subsequent PCR reaction. To minimize errors and the effect of sample-to-sample variation, RT-PCR is usually performed using an internal standard. The ideal internal standard is expressed at a constant level among different tissues, and is unaffected by the experimental treatment.

10   RNAs most frequently used to normalize patterns of gene expression are mRNAs for the housekeeping gene glyceraldehyde-3-phosphate-dehydrogenase (GAPDH), as used herein, or the ß-actin gene.

Although the PCR step can use a variety of thermostable DNA-dependent DNA polymerases, it typically employs the Taq DNA polymerase, which has a 5'-3' nuclease activity but lacks a 3'-5' proofreading endonuclease activity. Thus, TaqMan.RTM. PCR typically utilizes the 5'-nuclease activity

15   of Taq or Tth polymerase to hydrolyze a hybridization probe bound to its target amplicon, but any enzyme with equivalent 5' nuclease activity can be used. Two oligonucleotide primers are used to generate an amplicon typical of a PCR reaction. A third oligonucleotide, or probe, is designed to detect nucleotide sequence located between the two PCR primers. The probe is non-extendible by Taq DNA polymerase enzyme, and is labeled with a reporter fluorescent dye and a quencher fluorescent dye. Any

20   laser-induced emission from the reporter dye is quenched by the quenching dye when the two dyes are located close together as they are on the probe. During the amplification reaction, the Taq DNA polymerase enzyme cleaves the probe in a template-dependent manner. The resultant probe fragments disassociate in solution, and signal from the released reporter dye is free from the quenching effect of the second fluorophore. One molecule of reporter dye is liberated for each new molecule synthesized, and

25   detection of the unquenched reporter dye provides the basis for quantitative interpretation of the data.

TaqMan.RTM. RT-PCR can be performed using commercially available equipment, such as, for example, ABI PRISM 7700.TM. Sequence Detection System.TM. (Perkin-Elmer-Applied Biosystems, Foster City, Calif., USA), or Lightcycler (Roche Molecular Biochemicals, Mannheim, Germany). In a preferred embodiment, the 5' nuclease procedure is run on a real-time quantitative PCR device such as

30   the ABI PRISM 7700.TM. Sequence Detection System.TM.. The system consists of a thermocycler, laser, charge-coupled device (CCD), camera and computer. The system amplifies samples in a 96-well format on a thermocycler. During amplification, laser-induced fluorescent signal is collected in real-time through fiber optics cables for all 96 wells, and detected at the CCD. The system includes software for running the instrument and for analyzing the data.

- 14 -

A more recent variation of the RT-PCR technique is the real time quantitative PCR, which measures PCR product accumulation through a dual-labeled fluorigenic probe (i.e., TaqMan.RTM. probe). Real time PCR is compatible both with quantitative competitive PCR, where internal competitor for each target sequence is used for normalization, and with quantitative comparative PCR using a

5   normalization gene contained within the sample, or a housekeeping gene for RT-PCR. For further details see, e.g. Held et al., Genome Research 6:986-994 (1996).

The genes which are assayed according to the present invention are typically in the form of mRNA or reverse transcribed mRNA. The genes may be cloned or not and the genes may be amplified or not. The cloning itself does not appear to bias the representation of genes within a population. However,

10   it may be preferable to use polyA+RNA as a source, as it can be used with less processing steps. General methods for mRNA extraction are well known in the art and are disclosed in standard textbooks of molecular biology, including Ausubel et al., Current Protocols of Molecular Biology, John Wiley and Sons (1997). Methods for RNA extraction from paraffin embedded tissues are disclosed, for example, in Rupp and Locker, Lab Invest. 56:A67 (1987), and De Andrs et al., BioTechniques 18:42044 (1995). In

15   particular, RNA isolation can be performed using purification kit, buffer set and protease from commercial manufacturers, such as Qiagen, according to the manufacturer's instructions. Other commercially available RNA isolation kits include MasterPure.TM. Complete DNA and RNA Purification Kit (EPICENTRE.RTM., Madison, Wis.), and Paraffin Block RNA Isolation Kit (Ambion, Inc.). Total RNA from tissue samples can be isolated using RNA Stat-60 (Tel-Test). RNA prepared from

20   tumor can be isolated, for example, by cesium chloride density gradient centrifugation.

As is apparent to one of ordinary skill in the art, nucleic acid samples used in the methods and assays of the invention may be prepared by any available method or process. Methods of isolating total mRNA are also well known to those of skill in the art. For example, methods of isolation and purification of nucleic acids are described in detail in Chapter 3 of Laboratory Techniques in Biochemistry and

25   Molecular Biology: Hybridization With Nucleic Acid Probes, Part I Theory and Nucleic Acid Preparation, Tijssen, (1993) (editor) Elsevier Press. Such samples include RNA samples, but also include cDNA synthesized from a mRNA sample isolated from a cell or tissue of interest. Such samples also include DNA amplified from the cDNA, and an RNA transcribed from the amplified DNA. One of skill in the art would appreciate that it may be desirable to inhibit or destroy RNase present in homogenates

30   before homogenates can be used.

Biological samples may be of any biological tissue or fluid or cells from any organism as well as cells raised in vitro, such as cell lines and tissue culture cells. Frequently the sample will be a "clinical sample" which is a sample derived from a patient. Typical clinical samples include, but are not limited to, sputum, blood, blood-cells (e.g., white cells), tissue or fine needle biopsy samples, urine, peritoneal fluid,

and pleural fluid, or cells therefrom. Biological samples may also include sections of tissues, such as frozen sections or formalin fixed sections taken for histological purposes.

The following non-limiting examples are presented to better illustrate the invention.

Methods and Materials

5   The practice of the present invention will employ, unless otherwise indicated, conventional techniques of molecular biology (including recombinant techniques), microbiology, cell biology, and biochemistry, which are within the skill of the art. Such techniques are explained fully in the literature, such as, "Molecular Cloning: A Laboratory Manual", 2.sup.nd edition (Sambrook et al., 1989); "Oligonucleotide Synthesis" (M. J. Gait, ed., 1984); "Animal Cell Culture" (R. I. Freshney, ed., 1987);

10   "Methods in Enzymology" (Academic Press, Inc.); "Handbook of Experimental Immunology", 4.sup.th edition (D. M. Weir & C. C. Blackwell, eds., Blackwell Science Inc., 1987); "Gene Transfer Vectors for Mammalian Cells" (J. M. Miller & M. P. Calos, eds., 1987); "Current Protocols in Molecular Biology" (F. M. Ausubel et al., eds., 1987); and "PCR: The Polymerase Chain Reaction", (Mullis et al., eds., 1994).

15   Compounds: The structure of the small molecule KDR kinase inhibitors, Compound A and Compound B, used in the exemplification of the present invention are as follows:

Compound A

20

Compound B

25
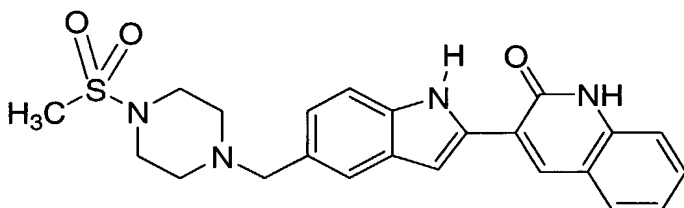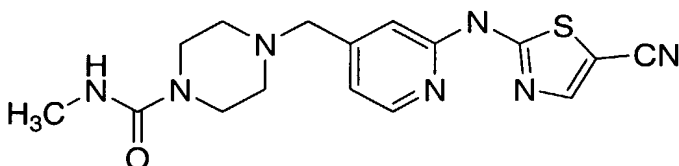
Cell Culture: Primary human dermal microvascular endothelial cells (HDMVEC) and rat heart microvascular endothelial cells (RHMVEC) were purchased from VEC Technologies (Renneslaer, NY) and grown in culture according to the supplier's directions. endothelial cell monolayers were maintained at 37°C in a 5% CO_2 humidified atmosphere in tissue culture flasks coated with human fibronectin

30   (Sigma, St. Louis, MO) using complete MCDB-131 media (MCDB-131 supplemented with 10% fetal

bovine serum (FBS, Invitrogen, Carlsbad, CA) and the growth factor cocktail ENDOGRO, VEC Technologies).

For *in vitro* MVEC proliferation experiments, cells were harvested by trypsinization between passage 3-6 following initiation of culture from frozen stocks, counted, and seeded in fibronectin-coated

5   tissue culture plates at 75% confluence (1.5 x 106 cells/per plate, 100 mm diameter plates). Cell growth was arrested for 24h by mitogen withdrawal and then stimulated by the addition of 100 ng/ml VEGF, 100 ng/ml bFGF or 200 μg/ml ENDOGRO. For growth arrest the culture media was changed to pre-warmed DMEM supplemented with 10% FBS. For stimulation of cell growth the growth arrest media was replaced with MDCB-131 supplemented with 10% FBS and the appropriate growth factor. Matched

10   control plates that received no supplemental stimulatory growth factor were made for each stimulation condition. At the desired time following growth factor stimulation, the culture media was removed quickly by aspiration, and the cells were lysed in 1.2 ml RLT buffer (guanidine thiocyanate lysis buffer for RNA stabilization and purification, QIAGEN, Valencia, CA). Cell lysates were homogenized in QIAshredders and total RNA was isolated with RNeasy MINI affinity columns (QIAGEN, Valencia,

15   CA). Gene expression profiles from a total of 8 independent VEGF-stimulated cultures, 7 ENDOGRO-stimulated cultures, and 4 bFGF-stimulated cultures were determined for HDMVECs. Profiles from 4 independent VEGF-stimulated cultures, 4 ENDOGRO-stimulated cultures, and 4 bFGF-stimulated cultures were determined For RHMVECs.

20   Animal Tumor Models: A rat glial cell line (C6, ATCC CCL-107) and a rat mammary adenocarcinoma (MatBIII, ATCC CRL-1666) were used for our animal tumor models. C6 cells were maintained in culture at 37°C in a 5% CO2 humidified atmosphere in Ham's F-12 medium supplemented with 2 mM L-glutamine, 1 mg/ml sodium bicarbonate, 15% horse serum, 2.5% fetal bovine serum, 10 U/ml penicillin, and 10 μg/ml streptomycin (all media components from Invitrogen). MatBIII cells were grown in

25   McCoy's 5a medium supplemented with 1.5 mM glutamine, 10% FBS 10 U/ml penicillin, and 10 μg/ml streptomycin. For RNA isolation from C6 or MatBIII cells, 2x106 cells growing in a 100 mm diameter tissue culture plate were lysed directly in 1.2 ml RLT buffer. Following lysate homogenization with a QIAshredder, total RNA was isolated with RNeasy MINI affinity columns.

C6 glial cells and MatBIII adenocarcinoma cells were chosen for animal models because they

30   were obtained from Fischer 344 (F344) rats and therefore could be used to create syngeneic tumors in immunocompetent F344 animals. Prior to implantation, cells were collected, washed in phosphate-buffered saline and resuspended in Hanks Balanced Saline Solution (Invitrogen) at a density of 2x107 (C6) or 2x106 (MatBIII) cells/ml.

<u>C6 glioma flank tumor model</u>: C6 cells were injected subcutaneously into the right flank of male F344 rats (150-175 g, 107 cells per animal). Following cell injection, animals were randomized according to body weight to receive either vehicle (0.5% methylcellulose) or drug (10 mpk/dose Compound B or 40 mpk/dose Compound A in 0.5% methylcellulose) (12-15). Once-daily oral dosing began 7 days post

5   tumor cell implantation and continued for 1, 2, or 3 days at which point the animals were sacrificed. The tumors were bisected with half preserved for RNA extraction by snap-freezing in liquid nitrogen and half fixed for histology or immunofluorescence microscopy. Five vehicle-treated and five compound-treated animals were sacrificed at each timepoint. RNA was extracted from tumor samples with RNeasy Mini columns according to standard protocols (QIAGEN). Briefly, frozen tumor samples were weighed,

10   placed in sample tubes containing RLT buffer (600 μl RLT per 30 mg tissue), and immediately homogenized for 10-20 seconds using a rotor/stator homogenizer. Total RNA was isolated from homogenized tissue lysate with RNeasy affinity columns, resuspended in DEPC-treated water and frozen at -80°C. RNAs from the five tumors in each vehicle-treated cohort were combined to form three reference RNA pools. RNAs isolated from each of the tumor samples from the five compound-treated

15   rats in each cohort were compared to the appropriate time-matched reference pool of RNA during microarray hybridization. In addition, RNA from individual vehicle treated rats was compared to time matched vehicle treated pool in order to assess inter-animal variability.

<u>MatBIII Breast Cancer Metastasis Model</u>: MatBIII cells between passage 20-30 were injected on the

20   mammary fat pad around the 4th left nipple (106 cells/animal) of female F344 rats (150-175 g). Prior to dosing, animals were randomized into groups according to tumor size and body weight. Once daily oral dosing of Compound A (40 mpk/dose formulated in 0.5% methylcellulose) or vehicle (0.5% methylcellulose) began on day 7 post tumor cell implantation and continued for 4 additional days. Six vehicle-treated and six compound-treated animals were sacrificed on day 11, four hrs after final dosing.

25   At the time of necropsy, tumors were weighed immediately upon removal. Half of each tumor was fixed in Zn-Tris for histology or immunofluorescence microscopy and the other half immediately snap frozen in liquid nitrogen for RNA extraction. Total RNA was isolated in the same manner as with the C6 tumor studies. RNAs from the vehicle-treated cohort were combined to form a control RNA pool. RNAs isolated from each of the tumor samples from the compound-treated rats was compared to the control

30   pool of RNA during microarray hybridization. RNAs from individual vehicle treated animals was compared to the vehicle treated pool in order to assess inter-animal variability.

<u>Gene Expression Profiling</u>: Total RNA isolated from cultured cells or tumor tissue samples was used to make fluorescently-labeled complementary RNA (cRNA) that was hybridized to DNA microarrays as

35   previously described (16, 17). Briefly, 4 μg total RNA from an individual tumor sample or *in vitro*

endothelial cell culture was used to synthesize double-stranded DNA through reverse transcription. cRNA was produced by *in vitro* transcription and labeled post-synthetically with Cy3 or Cy5. Two populations of labeled cRNA, a reference population and experimental population, were compared to each other by competitive hybridization to oligonucleotide arrays synthesized in situ with inkjet

5   technology. Two hybridizations were performed with each cRNA sample pair using a fluorescent dye reversal strategy. For animal tumor studies, reference cRNA pools were made by pooling equal amounts of cRNA from each tumor in the appropriate vehicle-dosed group. After hybridization, arrays were scanned and fluorescence intensities for each feature were recorded. Ratios of transcript abundance (experimental to control) were obtained following normalization and correction of the array intensity

10   data. Gene expression data analysis was performed with the Rosetta Resolver Client software (v3.2, Rosetta Biosciences, Kirkland, WA). A one-way ANOVA test was used to determine statistically significant changes in gene expression.

Quantitative real time PCR: Quantitative real time polymerase chain reaction was performed with gene-

15   specific PCR primer pairs and amplicon-specific fluorescent probes (TaqMan, Applied Biosystems Inc. (ABI), Foster City, CA) according to published protocols (ABI Assays-on-Demand™ Gene Expression Protocol, Rev A, http://docs.appliedbiosystems.com/pebiodocs/04333458.pdf). One-step quantitative reverse transcription PCR reactions were performed using ABI's TaqMan® One-Step RT-PCR Master Mix Reagents (ABI Product# 4309169) and 25 ng total RNA template on an ABI Prism 7900HT

20   Sequence Detection System. Two-step reverse transcription PCR experiments were initiated by cDNA synthesis from 25 ng total RNA as template using ABI's High Capacity cDNA Archive Kit (ABI Product# 4322171). Second step quantitative real time PCR was performed with standard reagents (TaqMan® Universal PCR Master Mix, ABI Product# 4324018) on the ABI Prism 7900HT Sequence Detection System. Real time PCR reactions were performed in duplicate in a 25 μl reaction volume in

25   384-well plates. Primer and probe sequences used for each gene are listed below. For every RNA sample, transcript abundance of GAPDH was determined.

In addition, transcript abundance of genes of interest and GAPDH were determined for calibrator RNA samples, either total human lung RNA or total rat lung RNA. Fold changes in gene expression were calculated using the $\Delta\Delta$CT method (ABI User Bulletin #2, Rev B: Relative Quantitation Of Gene

30   Expression, http://docs.appliedbiosystems.com/pebiodocs/04303859.pdf) The teachings of which are incorporated herein by reference.

The sequences of the individual biomarker genes which comprise the proliferation and expression signatures disclosed in tables 3-6 are readily available in public databases. The signatures defined in Tables 3 and 4 (HDMVEC and RHMVEC proliferation signatures, respectively) provide the

35   GenBank Accession Number and gene symbol for the included biomarkers, the sequences of which are

hereby incorporated by reference. The endothelial cell specific signatures defined in Tables 5 and 6 also provide the GenBank Accession Number and GeneSymbol for the biomarkers comprising the expression signature. The following list provides the name, Accession Number and primer and probes used to detect a subset of the biomarkers:

Hs refers to *Homo sapiens*. Rn refers to *Rattus norvegicus*.

Gene	RefSeq Acc#	Primer Sequence (or ABI Assay-on-Demand™ ID)
Angpt-2	XM_225004 (Rn)	

SEQ ID NO: 1	Forward Primer	5' - GAC AGA GTC CGA ATG CAT GCT - 3'
SEQ ID NO: 2	Reverse Primer	5' - TGC GGG TCT GGA GAA ATA CC - 3'
SEQ ID NO: 3	TaqMan Probe	5' - CCC TGT GAT TCT AAC CAT GGC CTT CTC A - 3'

	NM_001147 (Hs)	Hs00169867_m1

Ifit-3	XM_220059 (Rn)	

SEQ ID NO: 4	Forward Primer	5' - CGG TTG TTA TCA GGC TCA TAG GAT - 3'
SEQ ID NO: 5	Reverse Primer	5' - TGT GGG AGG CAA CAC GAT TT - 3'
SEQ ID NO: 6	TaqMan Probe	5' - TCA GGA ATA GGC TGC CTG CAC CCC - 3'

Fut-4	NM_022219 (Rn)	

SEQ ID NO: 7	Forward Primer	5' - GAC CGA AAC GTG GCT GTC TAT C - 3'
SEQ ID NO: 8	Reverse Primer	5' - GTG ATG TGC ACC GCA TAG CT - 3'
SEQ ID NO: 9	TaqMan Probe	5' - CCG CTA CTT CCA CTG GCG TCG G - 3'

	NM_002033 (Hs)	

SEQ ID NO: 10	Forward Primer	5' - AAT TGG GCT CCT GCA CAC – 3'
SEQ ID NO: 11	Reverse Primer	5' - CCA GGT GCT GCG AGT TCT C - 3'
SEQ ID NO: 12	TaqMan Probe	5' - TGG CCC GCT ACA AGT TCT ACC TGG CTT - 3'

Plau	NM_013085 (Rn)	Rn00565261_m1
	NM_002658 (Hs)	Hs00170182_m1

Clu	NM_012679 (Rn)	Rn00562081_m1
	NM_001831 (Hs)	Hs00156548_m1
Etb	NM_017333 (Rn)	Rn00569139_m1
	NM_000115 (Hs)	Hs00240752_m1
Cyr61	NM_031327 (Rn)	Rn00580055_m1
	NM_001554 (Hs)	Hs00155479_m1
GAPDH	NM_017008 (Rn)	4308313
GAPDH	NM_002046 (Hs)	402869

Immunohistochemistry: Tumor samples were fixed immediately upon removal from sacrificed animals by submersion in a Zn-Tris fixative solution for immunohistochemistry (IHC Zinc Fixative, BD Biosciences-Pharmingen, San Diego, CA) for 24 hr at room temperature (RT, 22°C) followed by submersion in 70% ethanol at RT for an additional 24 hrs. All subsequent steps were performed at RT. Tumor samples were embedded in paraffin (Tissue-Tek VIP Processing/Embedding Medium, Sakura Finetek, Torrance, CA) and cut into 3 μm sections on a Sakura Accu-Cut SRM microtome (Sakura Finetek). Tissue sections were de-waxed in xylene and re-hydrated through graded ethanol washes. Following washes in deionized H20 (dH20) and tris-buffered saline (TBS), a hydrophobic barrier was placed around the tissue section with a hydrophobic pen (Super Pap Pen, EMS #71310).

CD31 staining: CD31 is a validated endothelial cell-specific protein (18-20). Sections were blocked with Protein Block (Biogenex, San Ramon, CA) for 30 min and incubated with anti-CD31 antibodies (mouse anti-rat, Serotec, Raleigh, NC) diluted 1:1000 in DAKO Antibody Diluent with Blockers (DakoCytomation, Carpinteria, CA) for two hours. After several brief washes in TBST (TBS + 0.1% Tween-20), sections were incubated with biotinylated anti-Mouse IgG secondary antibody (DakoCytomation Alkaline Phosphatase Kit Link K-0610) for 10-30 min, washed several times with TBST, and incubated with streptavidin coupled to alkaline phosphatase (DAKO Alkaline Phosphatase Kit K-0610) for 10-30 min. Sections were then washed again with several changes of TBST and CD31 bound antibodies were visualized by incubation with Vulcan Fast Red Substrate (Biocare Medical, Walnut Creek, CA) for 10min (color development monitored microscopically). Sections were then washed in dH2O stored overnight in TBS.

Ki67 Staining: Ki67 is a validated nuclear protein expressed only in proliferating cells (21, 22). To facilitate antibody recognition of Ki67, we used a high temperature antigen retrieval strategy. Sections were submerged in Target Retrieval Solution (1x DakoCytomation S1699 diluted with dH2O) in a Decloaking Chamber (Biocare Medical, DC2002) and heated to 195°C for 1 min. Sections were cooled

5   with running dH2O into the retrieval solution and then rinsed in TBS. Residual peroxidase activity was blocked by incubating the sections with 3.0% H2O2 in TBS for 20 min. Sections were washed several times in TBS, then incubated with anti-Ki67 antibodies (rabbit anti-human, Novacastra, Newcastle upon Tyne, UK) diluted 1:2000 in antibody diluent for 2 hrs. Sections were washed with TBST, and then incubated with undiluted biotinylated anti-rabbit IgG (DakoCytomation, Link K-0609) for 10 min.

10 Sections were washed in TBST, and then incubated with streptavidin coupled to horseradish peroxidase (DakoCytomation, K0609) for 10 min. Sections were washed again in TBST, and antibodies bound to Ki67 were visualized by incubation with diaminobenzidine plus substrate (DakoCytomation, DAB+) for 5 min (color development monitored microscopically). Sections were washed in dH2O, incubated with DAB Enhance for 20 min RT, and washed again with dH2O. Tumor sections were counterstained with

15 filtered Mayer's Hematoxylin (Lillie's Formulation, DakoCytomation) for two min, and then washed with tap H2O until no color remained in the wash water. Sections were then rinsed in dH2O, dehydrated with 100% ethanol, cleared with xylenes and mounted with Permount (Fisher Scientific, Hampton, NH).

Immunohistochemical Analysis of Endothelial Cell Proliferation: Sequential brightfield images of

20 CD31/Ki67 double-labeled tumor sections were obtained with a 3-CCD color video camera (Optronics) attached to an Olympus BX-50 microscope equipped with an automated stage (Prior H128, Watertown, MA) and a 40x objective. The number of images per section varied between 1000 and 4000 depending on total tissue area. CD31 staining and Ki67 staining were quantitated for each image using the ImageProPlus software package (Media Cybernetics, Carlsbad, CA). Proliferating endothelial cells were

25 identified as those cells with cytoplasmic CD31 staining and nuclear Ki67 staining. Cells staining positive for CD31 but without nuclear staining for Ki67 were scored as non-proliferating endothelial cells. The percentage of proliferating endothelial cells was calculated by dividing the Ki67-positive nuclear area associated with endothelial cells by the total nuclear area associated with endothelial cells (both Ki67+ and Ki67-). Endothelial cell proliferation percentages represent the combined analysis

30 results from at least 100 images with CD31 staining per tumor section.

Immunofluorescence Microscopy: Tumor samples were fixed, embedded, sectioned, de-waxed, and re-hydrated as described for immunohistochemistry above. All subsequent steps were performed at room temperature. After a brief rinse in TBS, tissue sections were blocked by incubation with Sniper Blocking

35 Reagent (Biocare Medical) for 5-10 min, rinsed in TBS and incubated with primary antibodies diluted

1:1000 in DAKO Antibody Diluent for 2 hrs (Antibodies against ANGPT2, CLU, CYR61, and PLAU were from Santa Cruz Biotechnology, Santa Cruz, CA and were raised in goat or rabbit; antibodies against EDNRB were from Calbiochem, San Diego, CA and raised in sheep, antibodies against CD31 were from Serotec and raised in mouse). Sections were then washed with Tris-buffered saline containing

5   0.2% Tween-20 (TBST, Sigma) and incubated with appropriate secondary antibodies diluted 1:200 (10ug/ml) in DAKO Antibody Diluent with blocking serum for 45 min (Alexa Fluor 488 donkey anti-goat IgG, Alexa Fluor 488 goat anti-rabbit IgG, Alexa Fluor 488 donkey anti-sheep IgG, Molecular Probes, Eugene, OR; Normal donkey and normal goal blocking serum, Sigma). Following additional washes with TBST, sections were counterstained with DAPI (Molecular Probes, 1:2000 dilution of 1

10   mg/ml stock in MQH2O) for 30 min. Sections were then washed in TBST, dehydrated in 100% EtOH, cleared in xylene, and mounted under coverslips with Permount. Images were captured with a Zeiss Axiocam mHR CCD camera connected to a Zeiss Axiovert 135 inverted fluorescence microscope equipped with a 40x objective. For each fluorophore, all images were captured using equal camera integration times.

15

EXAMPLE 1   IDENTIFICATION OF GENE EXPRESSION CHANGES IN PROLIFERATING
                    MICROVASCULAR ENDOTHELIAL CELLS

        In order to identify genes that are regulated in proliferating endothelial cells relative to quiescent endothelial cells, we employed an *in vitro* angiogenesis model in which primary cultured microvascular

20   endothelial cells were driven to proliferate from a quiescent state by incubation with growth factors. Primary human dermal microvascular endothelial cells (HDMVECs) or rat heart microvascular endothelial cells (RHMVECs) between passage 4 and 7 were grown in monolayers in tissue culture dishes, mitogen-starved for 24 hr, then induced to proliferate by exposure to VEGF, bFGF, or ENDOGRO.

25   HDMVECs or RHMVECs were trypsinization following the third passage in culture and seeded in fibronectin-coated, six-well tissue culture plates at a density of 10,000 cells well. Cell growth was arrested for 24h by mitogen withdrawal and then stimulated by the addition of 100 ng/ml VEGF, 100 ng/ml bFGF or 200 μg/ml ENDOGRO. Wells with unstimulated cells and wells containing un-arrested cells were included as controls. At 72 hr following growth factor stimulation, cells were removed from

30   the culture plates by trypsinization and counted on a hemocytometer under bright-field microscopy.
        To confirm that VEGF, bFGF, and ENDOGRO (a bFGF-rich bovine brain extract, VEC Technologies) were signaling through different growth factor receptors, we exposed cells to VEGF, bFGF, or ENDOGRO in the presence of Compound A, which is small molecule KDR kinase inhibitor that is 100-fold less active against FGFR1 and FGFR2 (Table 1) (12-15).

35

	IC$_{50}$ (nM)	
Kinase	Compound A	Compound B
KDR	4.2	12
KDR (rat)	2.3	6.1
FLT1	124	251
FGFR1	511	1232
FGFR2	106	402
HUVEC mitogenesis	17	31

A comparison of the gene expression pattern of mitogen-starved, quiescent HDMVECs and
5   RHMVECs to the expression pattern of actively dividing endothelial cells, indicates significant
(p-value <0.01)gene expression changes, that are characteristic of proliferating vascular endothelial cells.
Briefly, endothelial cell cultures were grown in culture and mitogen deprived for 24 hr as described
above. Following a 24 hr stimulation with growth factor, culture media was aspirated quickly and the
cells lysed in an RNA stabilizing buffer. Matched control plates that received no supplemental
10   stimulatory growth factor were present for each stimulation condition and RNAs isolated from them
served as the reference to which the RNAs from the stimulated cells was compared.
Results: Although growth media supplemented with 10% FBS was not sufficient to drive endothelial cell
proliferation, 10% FBS plus additional growth factor induced rapid endothelial cell proliferation.
The data provided in Figure 1 demonstrates that exposure of HDMVEC (Figure 1A) and
15   RHMVEC (Figure 1B) to Compound A selectively inhibits *in vitro* microvascular endothelial cell
proliferation induced by VEGF as determined by viable cell counting with a hemocytometer. The gene
expression profile illustrated in Figure 2 graphically illustrates a gene expression signature that is
characteristic of proliferating HDMVEC (panel A) and RHMVEC (panel B) cultures. Color intensity
represents the degree of regulation, not mRNA copy number.
20   Table 3 provides a list of genes comprising the HDMVEC Proliferative Signature identified in
the expression profiles illustrated in Figure 2. Table 4 provides a list of genes comprising the RHMVEC
Proliferative Signature identified in the expression profiles illustrated in Figure 2. Using the information
provided in Tables 3 and 4 it is well within the abilities of a skilled artisan to design and validate a gene
expression-based assay that is suitable for evaluating the proliferation of vascular endothelial cells in
25   either *in vitro* or *in vivo* screening assay format.

EXAMPLE 2   SUPPRESSION OF VEGF-INDUCED GENE EXPRESSION SIGNATURES IN
            PRIMARY ENDOTHELIAL CELLS BY A KDR KINASE INHIBITOR

To determine if the growth factor-induced proliferation signatures identified in Example 1 are
sensitive to KDR kinase inhibitors, we stimulated HDMVECs or RHMVECs with VEGF or bFGF for 24
5   hrs in the presence of 100 nM Compound B. VEGF binds to and activates the fms-like tyrosine kinase
(FLT1) and KDR (23, 24). Both FLT1 and KDR are inhibited by Compound B (Table 1). bFGF binds to
FGFR1 and FGFR2, but not FLT1 or KDR. Both FGFR1 and FGFR2 are relatively insensitive to
Compound B (see Table 1).

Briefly, EC monolayers were maintained in complete MCDB-131 media until reaching ~75%
10   confluence, then induced into a quiescent state by mitogen starvation for 24 hr. Cells were then
stimulated to proliferate with 100 ng/ml VEGF for 24 hr in the presence or absence of Compound B.
RNA populations isolated from cells exposed to VEGF or VEGF + Compound B were compared to
matched control RNAs isolated from quiescent cells exposed to neither VEGF nor Compound B.
Results: The data provided in Figure 3 demonstrate that the HDMVEC VEGF-induced gene expression
15   signature was effectively suppressed by Compound B while the bFGF-induced signature was unaffected.
Parallel experiments were performed with RHMVECs (data not shown). Each point in the plots
represents a gene sequence present on the DNA oligonucleotide microarray and is plotted according to
the ratio of the two mRNA levels (experimental sample intensity:control sample intensity, vertical-axis)
and the total mRNA quantity (experimental sample intensity + control sample intensity, horizontal-axis)
20   for that gene.

EXAMPLE 3   IDENTIFICATION OF AN ENDOTHELIAL CELL-SPECIFIC
            PROLIFERATION SIGNATURE

The experimental data provided above identifies gene expression profiles, or expression
25   signatures specific for proliferating endothelial cells. However, the majority of genes regulated during
endothelial cell proliferation will also be expressed in other types of proliferating cells (genes that
regulate cell cycle and metabolic processes, for example). Tumors contain a complex mixture of cell
types, where approximately 1 in 2000 cells (0.05%) are proliferating endothelial cells (Joanne
Antanavage, Rosemary McFall, and Ken Thomas, personal communications). Therefore, in attempting
30   to develop a pharmacodynamic assay that specifically measure tumor endothelial cell proliferation, it was
acknowledged that there was a need to identify the endothelial cell-specific portion of the HDMVEC and
RHMVEC proliferation signatures. Candidate endothelial cell-specific genes were defined as genes
characterized by regulated expression during an *in vitro* proliferative response to mitogens, but
expressed at relatively low levels in non-endothelial cells.

We used microarray intensity data, which corresponds to the number of labeled cRNAs bound to each array feature and is proportional to mRNA copy number, from previous expression profiling studies and compared it with the microarray intensity data from our HDMVEC proliferation experiments. Existing intensity data from a panel of actively growing tumor-derived cell lines (MOLT-4, HL-60, Raji,

5   SW480, Daudi, G361, A549, K562, MCF7) was used to remove from consideration those genes with EC:tumor microarray intensity ratios less than 3:1.

702 HDMVEC sequences were selected as endothelial cell-specific in this manner (see, Table 3). We identified many known endothelial cell-specific genes by this method (i.e. ESM-1KDR, FLT-1) as well as numerous novel sequences. In parallel, we obtained a measure of endothelial cell specificity for

10 genes regulated in proliferating RHMVECs by comparing microarray intensity data from the RHMVEC experiments to data from gene expression profiling experiments with rat C6 glioma cells actively growing in culture. We identified 493 genes with RHMVEC:C6 intensity ratios greater than 3:1 (see, Table 4).

15 EXAMPLE 4   ORALLY-DOSED KDR KINASE INHIBITORS INDUCE SIGNIFICANT
             GENE EXPRESSION CHANGES IN SYNGENEIC ANIMAL TUMORS

Two syngeneic rat tumor models (i.e., C6 glioma flank tumor model and MatBIII Breast Cancer Metastasis Model), were used to assess the effect of the small molecule KDR kinase inhibitors, Compound A and Compound B, on thE genes identified as endothelial cell-specific which were regulated

20 during *in vitro* endothelial cell proliferation. Tumor studies were performed as described above in Materials and Methods. The tumor models use C6 glioma and MatBIII mammary carcinoma cell lines, both derived from Fischer 344 rats. These cell lines each secrete VEGF and form highly vascularized tumors that are sensitive to KDR kinase inhibitors.

Glioma Flank Tumor Model: C6 cells were injected subcutaneously into the right flank of rats and

25 allowed to form tumors for seven days. At that time, once-daily oral dosing with Compound A, Compound B, or vehicle commenced and continued for a total of 1, 2 or 3 days (Figure 4, Panel A "C6 Profiling Study). Figure 4 illustrates the growth kinetics of established rat tumors following exposure to a KDR kinase inhibitor. Tumor volumes were determined by caliper measurements. Tumors were calipered in two dimensions (length and width) and tumor volume was calculated according to the

30 formula (length) x (width) x (½ width).

Genome-wide gene expression in tumors isolated from compound-treated animals was compared to gene expression from tumors isolated from vehicle-treated animals. In the data provided in Figure 5 each row represents a distinct tumor from an individual animal. Each column represents a gene. Points corresponding to genes which are regulated (upregulated or downregulated) are indicated by various

35 shades of gray. The data presented in Panel A of Figure 5 identifies genes from rat C6 flank tumors that

are regulated following 24, 48, or 72 hrs of systemic exposure to the KDR kinase inhibitor Compound B. The data presented in Panel B of Figure 5 identifies genes from rat C6 flank tumors regulated following 24, 48, or 72 hrs of systemic exposure to the KDR kinase inhibitor Compound A.

5   We observed that both Compound A (Figure 5, Panel B) and Compound B (Figure 5, Panel A) induced robust gene expression changes in C6 tumor gene expression, particularly after 48 hrs or more of compound exposure (p-value < 0.05 for individual sequences).

MatBIII Breast Cancer Metastasis Model: MatBIII mammary adenocarcinoma cells were injected into a mammary fat pad of female rats. After allowing tumors to establish for seven days once-daily oral dosing of Compound A began and continued for a total of 5 days (Figure 4B). The data presented in Panel C of
10 Figure 5 identifies genes from rat MatBIII mammary tumors regulated following 100 hrs of systemic exposure to the KDR kinase inhibitor Compound A. When the pattern of tumor gene expression from compound-treated rats was compared to vehicle-treated controls, we again found significant differences (Figure 5, Panel C, p-value < 0.05 for individual sequences). While there was overlap in the gene expression changes induced by the KDR kinase inhibition between the three studies, the majority of gene
15 expression changes were study-specific (data not shown).

EXAMPLE 5   IDENTIFICATION OF GENE EXPRESSION BIOMARKERS OF
                  ENDOTHELIAL CELL PROLIFERATION

     In each of the three animal studies we performed, we found that we could detect KDR kinase
20 inhibitor-induced changes in expression for a fraction of those genes we had identified as specific to proliferating RHMVECs in culture. Figure 6 provides Venn diagrams which summarize the degree of overlap between the set of genes identified in the various assays formats disclosed herein. More specifically, Figure 6A summarizes the degree of overlap between the tumor gene expression responses to KDR kinase inhibitors in C6 flank tumors and MatBIII mammary tumors. Figure 6B indicates the
25 degree of overlap between the sets of endothelial cell-specific genes determined to be regulated both *in vitro* by mitogens and in tumor tissue by KDR kinase inhibitors. All genes/sequences represented in Panel B were observed to be regulated *in vivo* by KDR kinase inhibitors in a manner opposite that observed *in vitro* following exposure to mitogens.

     Most interestingly, we found in each study that some of those genes were regulated in a manner
30 consistent with suppression of endothelial cell proliferation. In effect, these genes were oppositely regulated in our *in vitro* proliferation experiments as compared to our *in vivo* tumor studies. In both cases the genes were highly expressed when endothelial cells were proliferating and expressed at low levels under non-proliferating conditions. Thus, we identified endothelial cell-specific genes that were "oppositely regulated" in each of the three animal tumor studies and identified genes that were regulated
35 as such in multiple studies (Figure 6B, and Tables 5 and 6). Tables 5 and 6 provide a list of genes which

were observed to be regulated by Compound A. Table 5 utilizes the data obtained in the C6 Flank Tumor and MatBill Breast Cancer Metatesis Models to define a Compound induced endothelial cell-specific expression signatures. The table provides the GeneBank Accession number, the gene symbol and summarizes the compound-induced fold change in gene expression that was observed. It is contemplated

5   that the expression signatures provided in Table 5 will find utility in evaluating the *in vivo* efficacy of anti-angiogenic agents in general and KDR kinase inhibitors in particular. Table 6 provides a summary of the changes (i.e., suppressed expression) observed for individual biomarkers comprising the EC-specific proliferation signatures disclosed herein in response to *in vivo* KDR inhibitor administration.

By imposing a requirement that genes to be considered as biomarkers should have compound-

10   induced *in vivo* expression changes of at least 1.6 fold, we identified seven genes that were "oppositely regulated" in both Compound A and Compound B studies and two genes that were "oppositely regulated" in all three studies. Based on the data provided in the instant disclosure, the seven genes (Angpt2, Ednrb, Plau, Clu, Fut4, Ifit3, and Cyr61) identified by both Compound A animal studies were identified as potential biomarkers for tumor endothelial cell proliferation. These genes are identified and

15   described in Table 2.

Table 2

Gene Symbol	RefSeq ID H. sapiens (R. norvegicus)	Gene/Protein Description
Angpt2	NM_001147 (XM_344544)	Angiopoietin-2. A Tie-2 ligand that functions in vascular remodeling.
Clu (ApoJ)	NM_001831 (NM_012679)	Clusterin/Apolipoprotein J. A secreted glycoprotein that associates with high-density lipoprotein that is implicated both as an anti-apoptotic and anti-proliferative.
Cyr61 (CCN1)	NM_001554 (NM_031327)	Cysteine rich protein 61/Cyr61,CTGF,NOV family member 1. A heparin binder, integrin $\alpha_V\beta_{3,5}$, $\alpha_M\beta_2$ ligand, and pro-angiogenic factor.
Endrb (EtB)	NM_000115 (NM_017333)	Endothelin receptor type B. A G-protein coupled receptor that mediates endothelin-induced vasoconstriction via the nitric oxide synthesis pathway.
Ifit3 (Garg-49)	NM_001549* (XM_220059)	Interferon-induced protein with tetratricopeptide repeats 3/ glucocorticoid-attenuated response gene 49. Function unknown. *RefSeq ID for Ifit4, the most similar human protein (60% identity, 78% similarity).
Fut4	NM_002033 (NM_022219)	Fucosyltransferase 4. An alpha 1,3-fucosyltransferase implicated developmental function, it is involved in the synthesis of myeloglycan, the major physiological ligand of E-selectin. It is highly expressed in some tumors with inverse correlation to prognosis.
Plau (uPA)	NM_002658 (NM_013085)	Urokinase type-plasminogen activator. A serine directed protease involved in vascular remodeling. It is a pro-tumor invasion and pro-metastasis factor.

Significantly, each of these genes has been reported to be involved or implicated in endothelial cell function.

Table. 3

HDMVEC Proliferation Signature

GenBank Accession Number	Gene Symbol	EC:MCF7 Intensity (Expression) Ratio	Fold Change	Growth Factor
AA013218	FLJ14079	6.81	1.33	ENDOGRO
AA029441		8.22	-1.17	VEGF
AA046478	NT5	4.48	1.35	ENDOGRO
AA053711	RBM8B	86.86	-1.38	ENDOGRO
AA053806	LOC64148	35.28	-1.45	ENDOGRO
AA102600		12.51	-1.51	bFGF
AA148511	FLJ22724	71.39	-1.18	bFGF
AA156672		28.11	1.51	ENDOGRO
AA166703		10.11	1.37	VEGF
AA173992		4.15	1.42	ENDOGRO
AA224245		14.16	-1.22	ENDOGRO
AA404374	FLJ21935	221.27	1.40	VEGF
AA449120		28.44	2.02	VEGF
AA464846		33.20	-1.34	VEGF
AA489383	BMP2	5.09	1.66	VEGF
AA522536		9.14	-1.55	bFGF
AA534774		3.09	-1.38	ENDOGRO
AA541787		12.99	-2.77	bFGF
AA584310		28.05	-1.36	ENDOGRO
AA617813		4.03	-1.35	VEGF
AA621714		8.79	-1.38	VEGF

AA628517		10.91	1.58	ENDOGRO
AA632012		12.16	-1.37	VEGF
AA707332		6.09	1.27	bFGF
AA740709		8.73	-1.72	ENDOGRO
AA758545	MMP2	93.44	-1.41	ENDOGRO
AA811265		10.22	-1.30	bFGF
AA815048	FLJ12649	4.37	-1.79	bFGF
AA858297		152.47	1.61	bFGF
AA868377	FLJ22233	3.66	1.45	ENDOGRO
AA868615		3.33	-2.01	bFGF
AA873008		8.82	-2.04	bFGF
AA897516		8.35	1.62	ENDOGRO
AA903334		29.77	1.57	ENDOGRO
AA923461		12.34	-1.30	ENDOGRO
AA932206		11.75	1.94	VEGF
AA946945		14.82	2.11	ENDOGRO
AB007954	KIAA0485	3.69	-1.44	VEGFD
AB011099	KIAA0527	104.01	-1.30	ENDOGRO
AB014538	KIAA0638	6.54	1.31	VEGF
AB014567	KIAA0667	3.53	-1.29	ENDOGRO
AB014604	KIAA0704	23.34	1.33	ENDOGRO
AB018301	KIAA0758	243.54	1.90	VEGF
AB018333	KIAA0790	3.12	1.57	ENDOGRO
AB018339	SYNE-1B	9.29	-1.44	bFGF
AB028019	LATS2	5.74	-1.43	ENDOGRO
AB028976	KIAA1053	11.78	-1.69	bFGF
AB028981	KIAA1058	6.73	1.24	VEGF
AB032971	KIAA1145	13.30	2.04	bFGF
AB033006	NDRG4	23.14	-1.79	VEGF
AB033035	KIAA1209	12.08	1.68	VEGF
AB033093	DKFZP727C091	4.05	-1.59	VEGFE
AB033100	KIAA1274	32.44	1.41	ENDOGRO
AB033101	KIAA1275	5.36	-1.86	bFGF
AB037722	KIAA1301	4.32	1.80	VEGF
AB037726	KIAA1305	5.96	-1.48	ENDOGRO
AB037751	KIAA1330	8.51	-1.42	ENDOGRO
AB037784	KIAA1363	3.50	1.65	ENDOGRO
AB037820	KIAA1399	289.61	-1.44	ENDOGRO
AB037821	PCDH10	8.07	-1.72	ENDOGRO
AB037857	KIAA1436	3.61	-1.16	ENDOGRO
AF007150		18.82	1.66	ENDOGRO
AF035121	KDR	70.01	1.39	bFGF
AF035306		12.18	-1.34	bFGF
AF035318		47.64	-1.68	bFGF
AF041037	SPRY1	10.05	1.90	VEGF
AF052169		83.10	-1.37	VEGF
AF061034	FIP2	8.51	-1.62	ENDOGRO

AF062341	CTNND1	5.61	-1.12	ENDOGRO
AF070569		4.62	-1.41	ENDOGRO
AF070641		8.76	4.19	ENDOGRO
AF091434	PDGFC	67.66	-1.37	ENDOGRO
AF095719	CPA4	19.14	-1.56	ENDOGRO
AF101051	CLDN1	3.73	-2.39	ENDOGRO
AF114264	unknown	35.87	-2.74	ENDOGRO
AF119663	LOC55970	6.47	-1.26	ENDOGRO
AF131762		4.22	1.34	ENDOGRO
AF131817		13.30	-1.49	VEGF
AF134404	FADS3	3.00	-1.58	ENDOGRO
AF181265	EHD4	5.55	1.09	ENDOGRO
AF186780	KIAA0959	14.14	1.53	VEGF
AF218942	FMN2	6.56	-1.75	bFGF
AF234532	MYO10	6.56	1.26	ENDOGRO
AF238083	SPHK1	4.48	1.37	ENDOGRO
AI005420		4.74	1.48	VEGFE
AI031794		7.72	-1.99	bFGF
AI039171		3.98	-1.33	ENDOGRO
AI051390		3.00	-1.32	ENDOGRO
AI052511		12.16	1.52	VEGF
AI073464	PLG	79.09	-1.25	ENDOGRO
AI073669		56.60	1.82	ENDOGRO
AI079944		5.90	1.44	VEGF
AI085787		29.37	3.06	VEGF
AI088104		8.74	-1.40	VEGF
AI125204		16.83	-2.15	bFGF
AI125425		7.25	1.68	ENDOGRO
AI139987	FLJ23056	32.76	-1.69	bFGF
AI141554		2709.99	-1.59	VEGF
AI141700	LOC63875	6.99	1.30	VEGFE
AI168436		7.67	-1.40	bFGF
AI188161		109.32	-2.23	bFGF
AI188513		3.42	1.27	ENDOGRO
AI200874		23.78	-1.45	ENDOGRO
AI203531	ART4	3.56	-2.05	ENDOGRO
AI206317		34.47	-1.39	ENDOGRO
AI208788		5.00	-2.02	bFGF
AI218538		20.83	-1.81	ENDOGRO
AI223799		3.29	-1.15	ENDOGRO
AI224533	DKFZp762L0311	3.19	1.70	ENDOGRO
AI275691		13.51	1.18	ENDOGRO
AI277316		4.21	-1.98	bFGF
AI291779		45.84	-1.44	VEGF
AI301312		6.62	-1.97	ENDOGRO
AI338631		11.26	-1.33	VEGFE
AI343000		8.60	-1.36	ENDOGRO

AI351898		14.00	1.13	ENDOGRO
AI357650	AD026	4.02	1.87	VEGF
AI375677		8.94	1.47	VEGF
AI376749	SDC2	5.18	-1.89	ENDOGRO
AI378647		6.03	-1.84	ENDOGRO
AI392987	HOXB6	4.40	1.44	ENDOGRO
AI418293		54.98	-1.34	VEGFE
AI418530		4.00	1.37	PIGF
AI418596		10.33	-1.62	bFGF
AI420933		54.00	-2.63	VEGF
AI433789	OS4	3.70	-1.44	ENDOGRO
AI433914		4.47	1.32	VEGF
AI439093		8.40	1.27	ENDOGRO
AI453557		24.20	-1.50	ENDOGRO
AI478770	MYH9	4.94	-1.39	ENDOGRO
AI479854	FLJ20980	46.10	-1.24	VEGF
AI498132		3.84	1.33	ENDOGRO
AI523391		3.67	-1.41	bFGF
AI539275		3.09	-1.22	VEGF
AI569689		3.53	-2.60	ENDOGRO
AI608902		17.83	-1.64	ENDOGRO
AI610727		4.23	-1.21	ENDOGRO
AI633826		5.30	3.89	VEGF
AI633890		48.69	-1.40	VEGF
AI635050	FLJ22252	327.52	-1.79	ENDOGRO
AI652289		31.67	1.32	ENDOGRO
AI652898		30.60	2.98	bFGF
AI652991		13.27	-1.76	ENDOGRO
AI654230		21.37	1.31	ENDOGRO
AI655345		9.29	1.47	ENDOGRO
AI659533	ARGBP2	108.45	-2.15	ENDOGRO
AI659800		4.82	-1.45	ENDOGRO
AI672407	HOXB8	3.72	2.26	bFGF
AI674404		7.93	1.21	bFGF
AI681538	FLJ23403	40.51	-1.48	VEGF
AI681805		15.66	-1.42	ENDOGRO
AI682468		3.07	-1.43	bFGF
AI683621		8.18	-1.77	bFGF
AI684489	CSF2RB	7.89	-1.59	ENDOGRO
AI684705		9.25	-1.29	VEGFE
AI688546	ARHGEF1	35.74	1.25	VEGFE
AI693178		22.73	-1.48	ENDOGRO
AI733194		5.60	-1.26	ENDOGRO
AI733570	FLJ20898	566.31	2.21	VEGF
AI739507	DAB2	1074.51	-1.73	ENDOGRO
AI741128		53.39	2.07	VEGF
AI741880		131.82	1.49	VEGF

AI742043		5.43	1.37	ENDOGRO
AI742210		4.99	1.28	ENDOGRO
AI742878		6.05	-1.77	VEGF
AI742936		8.15	1.23	ENDOGRO
AI743880		7.62	-1.36	ENDOGRO
AI743942		6.90	1.84	ENDOGRO
AI744591		31.91	1.34	ENDOGRO
AI745230		7.26	-1.52	VEGF
AI745614		27.20	-1.44	ENDOGRO
AI754423		83.30	-1.58	ENDOGRO
AI760613		6.16	-1.89	VEGF
AI765437		15.10	-1.55	ENDOGRO
AI767993		5.35	1.46	VEGF
AI769801	ALB	4.74	1.87	VEGF
AI803656		5.73	-1.27	ENDOGRO
AI806221		81.13	1.75	VEGF
AI806313	FLJ23091	34.79	-1.15	ENDOGRO
AI807266		6.54	1.46	ENDOGRO
AI810042	FLJ21841	16.31	1.44	ENDOGRO
AI822137		5583.85	-1.44	ENDOGRO
AI823801	SE57-1	5.65	1.35	ENDOGRO
AI825936	KIAA1350	12.43	1.42	ENDOGRO
AI827455		45.22	1.46	VEGF
AI828007		9.30	1.37	ENDOGRO
AI857683		3.74	1.27	VEGF
AI861824	SLC1A1	60.49	1.41	ENDOGRO
AI862120		6.44	-1.33	bFGF
AI887362		3.58	1.48	ENDOGRO
AI889160		5.58	-1.51	ENDOGRO
AI912975		71.62	-1.52	ENDOGRO
AI913402		75.58	-1.34	VEGF
AI924550		4.97	1.54	ENDOGRO
AI926697		6.91	1.67	ENDOGRO
AI927454		8.47	-1.14	ENDOGRO
AI927919		30.58	-1.27	ENDOGRO
AI928427		24.79	1.50	bFGF
AI936034		20.65	-1.58	ENDOGRO
AI949647		18.22	3.10	VEGF
AI949827		10.53	-1.63	bFGF
AI950109	FLJ12604	37.36	1.35	ENDOGRO
AI968085	WNT5A	3.31	-1.63	ENDOGRO
AI972337		6.36	1.65	ENDOGRO
AI979166		3.20	2.29	ENDOGRO
AI982765		10.21	-1.29	bFGF
AI992251		7.09	-1.36	bFGF
AK000401		4.30	-1.30	ENDOGRO
AK000711	TAX1BP1	12.69	-1.40	ENDOGRO

AK000776		110.22	-1.47	ENDOGRO
AK000884	LRRFIP1	17.73	1.26	VEGF
AK000959	FLJ10097	3.63	-1.19	ENDOGRO
AK001020		22.23	-1.37	bFGF
AK001362		3.02	-1.45	bFGF
AK001438	FBXL2	8.83	-1.33	VEGF
AK001560	LOC57863	16.74	-1.45	ENDOGRO
AK001630		126.78	1.38	VEGF
AK001872	PDL2	104.85	-1.24	bFGF
AK001903		11.23	-2.25	bFGF
AK001942		25.29	1.33	ENDOGRO
AK002195		6.46	1.31	VEGF
AL035306	STX12	4.35	-1.36	ENDOGRO
AL040051		6.17	-1.76	ENDOGRO
AL043980	PELI1	4.30	-1.28	ENDOGRO
AL049257		69.89	-1.59	ENDOGRO
AL049279		38.68	1.35	VEGF
AL049367		16.98	-1.38	VEGFE
AL049370		4.60	-1.99	ENDOGRO
AL049969		7.15	-1.70	ENDOGRO
AL049998		3.45	-1.17	ENDOGRO
AL050090	DKFZP586F1018	27.49	-1.25	ENDOGRO
AL050166		4.34	-1.37	ENDOGRO
AL110152		10.87	-1.20	ENDOGRO
AL110164		4.96	-1.52	ENDOGRO
AL110171		8.99	-1.30	VEGF
AL110202		4.31	-1.21	VEGF
AL110207		82.49	1.32	ENDOGRO
AL110255		4.30	-1.42	ENDOGRO
AL110280		7.38	-2.19	ENDOGRO
AL117427		4.11	-1.51	VEGF
AL117468	DKFZP586N1922	9.05	-1.51	ENDOGRO
AL117523	KIAA1053	15.24	-1.62	bFGF
AL117525	AKT3	32.46	-1.38	bFGF
AL117604	DLC1	15.23	-1.60	ENDOGRO
AL117615	DKFZP564D0764	257.68	-1.31	ENDOGRO
AL117617		4.04	1.32	bFGF
AL117664	DKFZP586L2024	117.73	-1.61	bFGF
AL122098	FLJ11937	3.98	-1.28	ENDOGRO
AL133118		30.13	1.63	VEGF
AL133596		12.02	-1.47	ENDOGRO
AL133605	PELI2	11.52	-1.71	bFGF
AL133640	DKFZp586C1021	4.67	-1.70	bFGF
AL133706		25.69	-1.39	VEGF
AL137540	NTN4	16.43	-1.86	ENDOGRO
AL137663		4.31	-1.46	bFGF
AL157431	DKFZp762A227	7.70	1.53	ENDOGRO

AL157475	DKFZp761G151	5.36	1.64	ENDOGRO
AL157482	FLJ23399	7.50	-1.57	ENDOGRO
AL157488		18.63	-1.45	VEGFE
AL157502	MSTP032	5.99	1.36	VEGF
AL359062		2726.41	-1.58	ENDOGRO
AL572015		4.16	-1.81	bFGF
AW015537		3.74	1.14	ENDOGRO
AW015898		11.49	-1.28	VEGF
AW023373		5.60	2.35	VEGF
AW024527		3.55	1.44	ENDOGRO
AW043571	FLJ20505	46.96	-1.63	ENDOGRO
AW069166	CALD1	275.85	-1.68	ENDOGRO
AW081929	KIAA1571	3.68	1.20	PIGF
AW102613		3.22	1.66	VEGF
AW117242		32.57	1.42	VEGF
AW119059		4.57	-1.60	bFGF
AW131552		8.49	2.99	VEGF
AW138207	FLJ22969	6.39	4.22	bFGF
AW139097		95.87	-1.21	ENDOGRO
AW139393	FTH1	37.66	1.63	ENDOGRO
AW139567		32.44	-1.70	ENDOGRO
AW139834		7.44	-1.43	VEGF
AW151025	ARHE	7.93	-1.92	ENDOGRO
AW173150		4.05	1.55	ENDOGRO
AW183161		42.71	-1.27	ENDOGRO
AW189467		3.79	-1.40	ENDOGRO
AW190823	LOC58514	4.54	1.57	ENDOGRO
AW195720		20.83	1.41	VEGF
AW237511		181.16	-2.84	VEGF
AW242009		4.21	1.42	ENDOGRO
AW243046		14.10	1.37	ENDOGRO
AW269515	FLJ20481	13.01	-1.61	ENDOGRO
AW269818	FLJ23144	7.49	-1.40	VEGF
AW271825		45.27	1.33	VEGF
AW274396		3.22	-1.11	ENDOGRO
AW274929		12.68	2.37	ENDOGRO
AW276078		24.62	1.61	bFGF
AW291331		16.15	-1.68	bFGF
AW291988		556.06	1.26	VEGF
AW292303		3.41	1.40	ENDOGRO
AW292755		8.16	1.28	VEGF
AW293366		3.66	-1.32	ENDOGRO
AW293770		1515.01	-1.50	ENDOGRO
AW294011		13.79	-1.41	ENDOGRO
AW294653	MOX2	20.80	1.68	VEGF
AW995919	PRG2	5.74	-1.26	ENDOGRO
BC005133		45.68	1.25	bFGF

BM263824		7.39	1.48	ENDOGRO
D38522	KIAA0080	31.39	-1.47	ENDOGRO
D43636	KIAA0096	9.12	1.77	bFGF
D50406	RECK	60.03	-1.30	ENDOGRO
G26403	LOC64148	15.13	-1.30	ENDOGRO
H05089	FLJ14033	11.27	-1.25	ENDOGRO
H09749		8.90	-1.78	bFGF
H11724		8.28	-1.21	ENDOGRO
H16409		28.49	-1.22	ENDOGRO
H56091		5.97	-1.81	bFGF
H80726		5.53	1.57	VEGF
M12758	HLA-A	4.93	-1.34	bFGF
M26383	IL8	91.08	1.30	VEGFE
M60721	HLX1	49.44	5.23	VEGFE
M68874	PLA2G4A	176.88	-1.18	ENDOGRO
M80783	TNFAIP1	3.66	-1.41	ENDOGRO
M90657	TM4SF1	17.14	1.26	ENDOGRO
M93718	NOS3	34.51	1.59	ENDOGRO
N36156		31.71	1.63	VEGF
N92500		4.02	1.16	bFGF
N92541	FLJ23462	7.63	-1.46	ENDOGRO
N95435		16.21	-1.73	bFGF
N99256	FLJ11808	4.58	-1.29	VEGF
NM_000019	ACAT1	3.04	-1.25	PlGF
NM_000024	ADRB2	27.96	1.94	ENDOGRO
NM_000089	COL1A2	16.78	-2.59	bFGF
NM_000093	COL5A1	4.58	-1.39	ENDOGRO
NM_000109	DMD	3.44	-1.73	VEGF
NM_000115	EDNRB	5.52	1.43	ENDOGRO
NM_000124	ERCC6	5.51	-1.40	VEGF
NM_000138	FBN1	38.80	-1.48	ENDOGRO
NM_000143	FH	3.13	-1.53	ENDOGRO
NM_000165	GJA1	636.59	-1.50	ENDOGRO
NM_000170	GLDC	3.21	1.60	ENDOGRO
NM_000201	ICAM1	5.70	-2.41	bFGF
NM_000204	IF	3.96	1.42	ENDOGRO
NM_000210	ITGA6	15.87	2.14	VEGF
NM_000237	LPL	9.12	-1.95	bFGF
NM_000240	MAOA	5.87	-2.02	ENDOGRO
NM_000304	PMP22	13.23	1.22	ENDOGRO
NM_000361	THBD	5.73	1.56	bFGF
NM_000393	COL5A2	20.35	-1.51	ENDOGRO
NM_000416	IFNGR1	4.03	-1.30	ENDOGRO
NM_000428	LTBP2	90.66	-1.42	VEGF
NM_000436	OXCT	3.56	-1.46	ENDOGRO
NM_000439	PCSK1	76.58	1.35	ENDOGRO
NM_000441	SLC26A4	5.08	1.89	VEGF

NM_000450	SELE	12.46	-3.51	bFGF
NM_000552	VWF	359.59	-1.26	bFGF
NM_000584	IL8	465.02	1.30	VEGFE
NM_000596	IGFBP1	17.07	1.50	bFGF
NM_000627	LTBP1	6.90	-1.14	ENDOGRO
NM_000689	ALDH1A1	133.54	-1.34	PIGF
NM_000784	CYP27A1	5.82	-1.35	ENDOGRO
NM_000793	DIO2	5.13	-1.87	VEGF
NM_000820	GAS6	22.28	-1.37	bFGF
NM_000824	GLRB	27.89	-1.41	ENDOGRO
NM_000885	ITGA4	20.27	-2.03	bFGF
NM_000902	MME	7.99	1.44	bFGF
NM_000919	PAM	3.37	-1.29	ENDOGRO
NM_000929	PLA2G5	3.66	-1.78	bFGF
NM_000930	PLAT	15.88	1.87	bFGF
NM_000931	PLAT	17.20	1.90	bFGF
NM_000950	PRRG1	9.96	-1.48	ENDOGRO
NM_000958	PTGER4	4.64	1.54	ENDOGRO
NM_000963	PTGS2	233.39	-2.13	ENDOGRO
NM_001066	TNFRSF1B	23.17	-1.38	VEGF
NM_001078	VCAM1	61.45	-7.79	ENDOGRO
NM_001122	ADFP	17.09	-1.32	VEGF
NM_001147	ANGPT2	9.05	3.98	VEGF
NM_001159	AOX1	5.24	1.68	ENDOGRO
NM_001165	BIRC3	3.66	-2.59	bFGF
NM_001166	BIRC2	4.58	-1.30	ENDOGRO
NM_001202	BMP4	14.66	-1.92	ENDOGRO
NM_001223	CASP1	23.83	-1.37	bFGF
NM_001290	LDB2	63.23	1.33	VEGF
NM_001336	CTSZ	41.31	1.63	VEGFE
NM_001343	DAB2	381.87	-1.77	ENDOGRO
NM_001399	ED1	3.60	1.40	ENDOGRO
NM_001430	EPAS1	5.28	-1.25	ENDOGRO
NM_001442	FABP4	7.69	2.05	VEGF
NM_001444	FABP5	9.91	1.50	ENDOGRO
NM_001450	FHL2	4.24	-1.41	VEGF
NM_001457	FLNB	3.39	-1.46	bFGF
NM_001613	ACTA2	11.65	-1.39	VEGF
NM_001627	ALCAM	7.03	-1.98	ENDOGRO
NM_001674	ATF3	4.18	-3.56	ENDOGRO
NM_001709	BDNF	357.01	-2.53	bFGF
NM_001711	BGN	3.05	-1.31	ENDOGRO
NM_001718	BMP6	66.96	-1.33	ENDOGRO
NM_001721	BMX	144.68	1.37	ENDOGRO
NM_001724	BPGM	13.36	-1.40	PIGF
NM_001773	CD34	310.68	-1.28	ENDOGRO
NM_001797	CDH11	17.51	1.32	bFGF

NM_001839	CNN3	243.45	-1.39	ENDOGRO
NM_001845	COL4A1	20.78	-1.32	ENDOGRO
NM_001850	COL8A1	74.23	-1.60	ENDOGRO
NM_001885	CRYAB	5.53	-1.53	ENDOGRO
NM_001924	GADD45A	3.89	-1.46	bFGF
NM_001945	DTR	38.30	-1.94	bFGF
NM_001946	DUSP6	32.18	2.13	ENDOGRO
NM_001955	EDN1	52.88	-1.74	ENDOGRO
NM_001992	F2R	83.85	-1.62	ENDOGRO
NM_002006	FGF2	34.80	-1.55	ENDOGRO
NM_002019	FLT1	88.72	2.54	VEGF
NM_002053	GBP1	6.07	-1.94	ENDOGRO
NM_002131	HMGIY	5.99	1.70	ENDOGRO
NM_002133	HMOX1	3.75	1.38	ENDOGRO
NM_002153	HSD17B2	32.56	2.49	bFGF
NM_002165	ID1	6.91	1.60	bFGF
NM_002185	IL7R	38.68	-1.31	ENDOGRO
NM_002189	IL15RA	8.70	1.53	ENDOGRO
NM_002192	INHBA	8.93	-2.11	bFGF
NM_002210	ITGAV	4.70	-2.03	ENDOGRO
NM_002223	ITPR2	5.74	-1.46	ENDOGRO
NM_002313	ABLIM	5.35	-1.46	ENDOGRO
NM_002341	LTB	5.48	-1.17	bFGF
NM_002350	LYN	6.10	1.37	VEGF
NM_002397	MEF2C	3.31	2.13	VEGF
NM_002402	MEST	3.13	-1.61	VEGF
NM_002421	MMP1	18.54	2.29	VEGF
NM_002425	MMP10	12.05	1.63	VEGF
NM_002438	MRC1	34.54	-1.35	ENDOGRO
NM_002451	MTAP	40.27	1.48	bFGF
NM_002475	MYL1	3.19	-1.13	ENDOGRO
NM_002526	NT5	5.84	1.73	VEGF
NM_002575	SERPINB2	47.87	3.04	ENDOGRO
NM_002595	PCTK2	4.39	1.28	ENDOGRO
NM_002599	PDE2A	10.28	1.61	ENDOGRO
NM_002600	PDE4B	12.97	1.60	ENDOGRO
NM_002608	PDGFB	11.22	-1.47	bFGF
NM_002659	PLAUR	6.03	2.16	bFGF
NM_002662	PLD1	11.32	-1.42	ENDOGRO
NM_002763	PROX1	6.17	1.69	ENDOGRO
NM_002837	PTPRB	102.95	-1.47	ENDOGRO
NM_002845	PTPRM	36.50	-1.27	bFGF
NM_002923	RGS2	12.21	2.02	ENDOGRO
NM_002933	RNASE1	25.36	-1.22	ENDOGRO
NM_002937	RNASE4	28.30	-1.49	ENDOGRO
NM_002982	SCYA2	10.53	-3.48	ENDOGRO
NM_002993	SCYB6	5.70	-2.66	bFGF

NM_002996	SCYD1	14.41	-5.15	ENDOGRO
NM_003003	SEC14L1	5.78	-1.13	ENDOGRO
NM_003082	SNAPC1	4.43	-1.60	VEGF
NM_003113	SP100	4.98	-1.58	ENDOGRO
NM_003115	UAP1	9.18	-1.37	VEGF
NM_003186	TAGLN	36.78	-1.67	VEGF
NM_003199	TCF4	181.64	1.22	VEGFE
NM_003238	TGFB2	9.39	-2.64	bFGF
NM_003246	THBS1	78.99	-1.77	bFGF
NM_003266	TLR4	18.63	-1.44	ENDOGRO
NM_003289	TPM2	7.89	-1.32	ENDOGRO
NM_003330	TXNRD1	5.26	-1.74	bFGF
NM_003459	SLC30A3	3.97	-1.73	bFGF
NM_003483	HMGIC	55.41	3.05	bFGF
NM_003494	DYSF	84.07	1.48	VEGF
NM_003603	ARGBP2	11.04	-1.90	ENDOGRO
NM_003607	PK428	3.85	-1.24	ENDOGRO
NM_003633	ENC1	3.48	-1.89	VEGF
NM_003662	PIR	3.05	-1.25	VEGF
NM_003676	DEGS	5.23	1.07	ENDOGRO
NM_003693	SREC	232.16	1.34	ENDOGRO
NM_003706	PLA2G4C	13.06	-2.90	bFGF
NM_003798	CTNNAL1	4.07	-1.23	ENDOGRO
NM_003810	TNFSF10	3.21	-2.50	VEGFE
NM_003812	ADAM23	18.65	-1.34	VEGF
NM_003816	ADAM9	6.16	-1.36	ENDOGRO
NM_003914	CCNA1	10.33	1.31	ENDOGRO
NM_003919	SGCE	8.43	-1.17	ENDOGRO
NM_003947	HAPIP	18.68	1.65	bFGF
NM_003956	CH25H	7.43	-3.03	bFGF
NM_003965	CCRL2	8.41	2.00	bFGF
NM_003975	SH2D2A	3.60	1.33	bFGF
NM_003991	EDNRB	5.28	1.39	ENDOGRO
NM_004010	DMD	5.12	-1.90	bFGF
NM_004024	ATF3	4.83	-4.15	bFGF
NM_004105	EFEMP1	23.60	-1.39	ENDOGRO
NM_004126	GNG11	3428.47	1.47	ENDOGRO
NM_004155	SERPINB9	5.22	1.16	ENDOGRO
NM_004156	PPP2CB	3.27	-1.20	ENDOGRO
NM_004159	PSMB8	10.81	-1.19	bFGF
NM_004184	WARS	4.49	-1.89	bFGF
NM_004267	CHST2	86.99	2.83	bFGF
NM_004289	NFE2L3	6.65	-1.49	VEGF
NM_004334	BST1	165.62	-1.96	bFGF
NM_004342	CALD1	120.74	-1.64	ENDOGRO
NM_004385	CSPG2	14.18	-1.75	VEGF
NM_004414	DSCR1	7.74	2.13	VEGF

NM_004417	DUSP1	5.71	1.53	bFGF
NM_004454	ETV5	16.90	2.73	ENDOGRO
NM_004490	GRB14	3.77	1.66	ENDOGRO
NM_004556	NFKBIE	4.86	-1.41	bFGF
NM_004609	TCF15	30.48	1.72	bFGF
NM_004675	ARHI	31.17	-1.47	ENDOGRO
NM_004791	ITGBL1	7.10	-1.40	ENDOGRO
NM_004796	NRXN3	5.25	-1.24	PIGF
NM_004808	NMT2	13.11	-1.73	bFGF
NM_004811	LPXN	3.02	1.36	ENDOGRO
NM_004877	GMFG	127.79	1.49	VEGF
NM_004881	PIG3	7.60	-1.15	ENDOGRO
NM_004895	C1orf7	3.19	1.64	ENDOGRO
NM_005012	ROR1	62.08	-1.64	VEGF
NM_005045	RELN	10.98	-1.42	ENDOGRO
NM_005072	SLC12A4	10.32	-1.48	ENDOGRO
NM_005100	AKAP12	152.34	1.62	VEGF
NM_005118	TNFSF15	3.83	-1.64	VEGF
NM_005127	CLECSF2	16.36	1.73	bFGF
NM_005168	ARHE	6.11	-1.69	ENDOGRO
NM_005203	COL13A1	3.85	1.31	ENDOGRO
NM_005238	ETS1	3.48	1.49	VEGF
NM_005282	GPR4	8.75	2.25	ENDOGRO
NM_005308	GPRK5	12.51	1.53	bFGF
NM_005360	MAF	5.11	-2.52	bFGF
NM_005420	STE	64.47	-2.17	bFGF
NM_005429	VEGFC	11.68	1.91	VEGF
NM_005438	FOSL1	3.17	1.71	ENDOGRO
NM_005460	SNCAIP	5.44	2.20	VEGF
NM_005541	INPP5D	40.84	1.40	ENDOGRO
NM_005556	KRT7	3.46	-1.17	ENDOGRO
NM_005574	LMO2	14.62	1.35	VEGF
NM_005585	MADH6	3.60	-1.38	VEGF
NM_005627	SGK	27.82	-1.17	ENDOGRO
NM_005630	SLC21A2	102.05	-1.39	ENDOGRO
NM_005711	EDIL3	10.36	-1.35	ENDOGRO
NM_005755	EBI3	3.54	-1.65	ENDOGRO
NM_005795	CALCRL	12.74	1.96	VEGF
NM_005953	MT2A	12.90	1.21	ENDOGRO
NM_005965	MYLK	3.93	-1.37	ENDOGRO
NM_006006	ZNF145	14.58	-2.00	bFGF
NM_006074	STAF50	74.18	-1.43	bFGF
NM_006094	DLC1	9.76	-1.69	ENDOGRO
NM_006100	ST3GALVI	26.24	1.42	VEGF
NM_006102	PGCP	8.16	-1.43	ENDOGRO
NM_006169	NNMT	530.16	-1.79	ENDOGRO
NM_006226	PLCE	13.52	1.64	ENDOGRO

NM_006227	PLTP	4.50	-1.33	bFGF
NM_006255	PRKCH	4.77	-1.18	ENDOGRO
NM_006320	PMBP	3.38	-1.33	ENDOGRO
NM_006398	UBD	33.18	-5.18	bFGF
NM_006404	PROCR	52.74	1.20	bFGF
NM_006407	JWA	3.65	-1.19	ENDOGRO
NM_006454	MAD4	3.47	-1.39	ENDOGRO
NM_006457	LIM	6.95	-1.73	ENDOGRO
NM_006474	T1A-2	9.84	1.45	bFGF
NM_006475	OSF-2	870.46	-1.34	bFGF
NM_006509	RELB	4.29	-2.33	bFGF
NM_006528	TFPI2	11.72	3.00	bFGF
NM_006691	XLKD1	5.82	2.91	bFGF
NM_006719	ABLIM	6.08	-1.43	ENDOGRO
NM_006729	DIAPH2	5.11	-1.34	ENDOGRO
NM_006779	CEP2	4.35	1.32	ENDOGRO
NM_006834	RAB32	3.33	-1.38	VEGF
NM_006855	KDELR3	3.47	-1.40	bFGF
NM_006905	PSG1	3.03	-1.49	VEGF
NM_006988	ADAMTS1	24.94	2.05	ENDOGRO
NM_007005	BCE-1	3.54	-1.32	VEGF
NM_007021	DEPP	3.11	1.64	VEGF
NM_007034	DNAJB4	53.46	-1.28	VEGF
NM_007066	PKIG	4.23	1.33	ENDOGRO
NM_007283	HU-K5	14.74	-1.39	bFGF
NM_007288	MME	7.05	1.44	bFGF
NM_007289	MME	5.59	1.41	bFGF
NM_007308	SNCA	120.69	-1.16	ENDOGRO
NM_007361	NID2	22.18	3.23	VEGF
NM_009588	LTB	5.38	-1.19	bFGF
NM_012082	FOG2	10.62	-1.25	ENDOGRO
NM_012250	TC21	9.43	-1.29	VEGF
NM_012269	HYAL4	5.99	-2.44	bFGF
NM_012323	MAFF	3.56	1.25	VEGF
NM_012449	STEAP	301.60	1.45	ENDOGRO
NM_013231	FLRT2	1584.59	-1.71	ENDOGRO
NM_013250	ZNF215	4.12	2.11	ENDOGRO
NM_013352	SART-2	7.17	-1.93	bFGF
NM_013372	CKTSF1B1	19.71	1.44	bFGF
NM_013423	ARHGAP6	8.68	2.49	VEGF
NM_013956	NRG1	29.07	-1.81	VEGF
NM_013957	NRG1	8.43	-1.74	VEGF
NM_013958	NRG1	13.34	-1.44	VEGF
NM_013961	NRG1	3.70	-1.37	VEGF
NM_013962	NRG1	20.39	-1.38	VEGF
NM_013989	DIO2	7.84	-2.07	VEGF
NM_014029	HSPC022	32.99	1.25	ENDOGRO

NM_014059	RGC32	28.92	-1.65	ENDOGRO
NM_014074	PRO0529	4.39	-1.42	VEGF
NM_014143	B7-H1	9.24	-1.30	VEGF
NM_014331	SLC7A11	16.15	-1.61	ENDOGRO
NM_014344	FJX1	7.64	1.39	ENDOGRO
NM_014349	APOL3	11.47	-1.43	bFGF
NM_014363	SACS	13.77	-1.44	VEGFE
NM_014391	CARP	46.40	-1.80	ENDOGRO
NM_014397	NEK6	3.95	-1.28	ENDOGRO
NM_014398	LAMP3	15.90	-1.35	ENDOGRO
NM_014465	ST1B2	39.94	-1.84	ENDOGRO
NM_014476	ALP	15.82	-1.19	ENDOGRO
NM_014521	SH3BP4	3.55	-1.52	ENDOGRO
NM_014570	ARFGAP1	3.13	-1.17	ENDOGRO
NM_014585	SLC11A3	46.27	-1.41	VEGFE
NM_014634	KIAA0015	7.30	1.52	bFGF
NM_014686	KIAA0355	3.24	-1.27	ENDOGRO
NM_014705	KIAA0716	87.07	1.36	ENDOGRO
NM_014721	KIAA0680	3.70	1.43	VEGF
NM_014731	KIAA0552	3.25	-1.79	ENDOGRO
NM_014737	RASSF2	23.65	1.40	ENDOGRO
NM_014782	KIAA0512	22.06	-1.38	ENDOGRO
NM_014795	ZFHX1B	158.26	-1.36	VEGF
NM_014822	SEC24D	3.59	-1.32	ENDOGRO
NM_014832	KIAA0603	3.75	1.56	VEGF
NM_014840	KIAA0537	7.79	-1.77	ENDOGRO
NM_014890	DOC1	12.99	-2.25	ENDOGRO
NM_014909	KIAA1036	5.45	1.42	VEGF
NM_014933	KIAA0905	3.78	-1.20	ENDOGRO
NM_014945	KIAA0843	4.21	1.20	ENDOGRO
NM_014959	KIAA0955	7.96	1.84	ENDOGRO
NM_014965	KIAA1042	4.04	-1.44	bFGF
NM_015376	KIAA0846	9.01	2.98	VEGF
NM_015675	GADD45B	3.51	-1.94	ENDOGRO
NM_015881	DKK3	286.01	-1.24	ENDOGRO
NM_016061	LOC51646	3.01	-1.64	ENDOGRO
NM_016109	PGAR	31.81	-1.99	VEGF
NM_016134	LOC51670	4.61	-1.36	ENDOGRO
NM_016203	PRKAG2	5.09	-1.22	VEGF
NM_016232	IL1RL1	15.56	-1.40	VEGF
NM_016235	GPRC5B	5.37	-1.53	bFGF
NM_016270	KLF2	5.53	2.17	bFGF
NM_016274	LOC51177	5.28	-1.48	ENDOGRO
NM_016352	CPA4	54.01	-1.55	ENDOGRO
NM_016357	EPLIN	4.98	-1.30	VEGF
NM_016385	HSPC057	4.00	-1.40	ENDOGRO
NM_016602	GPR2	4.94	-1.29	ENDOGRO

NM_016619	LOC51316	5.50	-1.38	ENDOGRO
NM_016848	SHC3	41.19	-1.31	VEGF
NM_016931	NOX4	80.07	1.17	ENDOGRO
NM_017415	KLHL3	40.42	1.72	ENDOGRO
NM_017577	DKFZp434C0328	3.90	-1.35	ENDOGRO
NM_017585	SLC2A6	8.27	-1.47	ENDOGRO
NM_017596	KIAA0449	3.45	1.41	ENDOGRO
NM_017718	FLJ20220	5.02	1.32	ENDOGRO
NM_017734	FLJ20271	124.25	-1.32	ENDOGRO
NM_017752	FLJ20298	6.73	-1.46	ENDOGRO
NM_017805	FLJ20401	41.04	1.27	ENDOGRO
NM_017905	FLJ20623	3.11	-1.30	ENDOGRO
NM_017980	FLJ10044	125.20	-1.42	ENDOGRO
NM_018004	FLJ10134	17.08	-1.46	bFGF
NM_018012	FLJ10157	3.96	-1.59	VEGF
NM_018057	FLJ10316	8.37	-1.52	ENDOGRO
NM_018071	FLJ10357	3.71	-1.59	bFGF
NM_018159	FLJ10628	6.29	1.17	ENDOGRO
NM_018192	FLJ10718	154.28	-2.02	bFGF
NM_018295	FLJ11000	4.10	-1.43	ENDOGRO
NM_018324	FLJ11106	5.31	-1.97	bFGF
NM_018326	FLJ11110	64.14	1.66	bFGF
NM_018357	FLJ11196	4.28	-1.34	ENDOGRO
NM_018370	FLJ11259	6.87	-1.49	ENDOGRO
NM_018384	FLJ11296	11.26	2.13	bFGF
NM_018401	HSA250839	3.61	1.19	bFGF
NM_018413	C4ST	3.30	1.51	ENDOGRO
NM_018476	HBEX2	106.48	-1.62	VEGF
NM_018482	DDEF1	3.45	-1.19	ENDOGRO
NM_018567	TNS	5.72	1.43	ENDOGRO
NM_018841	LOC55970	12.04	-1.33	ENDOGRO
NM_019858	A	14.27	1.21	ENDOGRO
NM_020130	C8orf4	22.69	-3.60	ENDOGRO
NM_020152	C21orf7	4.33	1.87	VEGF
NM_020163	LOC56920	30.25	-5.28	VEGFE
NM_020186	DC11	25.99	1.58	ENDOGRO
NM_020190	HNOEL-iso	3.76	-1.55	bFGF
NM_020353	LOC57088	426.58	-1.52	VEGF
NM_020651	PELI1	3.43	-1.38	bFGF
NM_021069	ARGBP2	192.99	-2.09	ENDOGRO
NM_021106	RGS3	9.55	-2.34	ENDOGRO
NM_021154	PSA	5.38	1.61	ENDOGRO
NM_021226	LOC58504	6.03	1.38	ENDOGRO
NM_021255	PELI2	6.20	-1.77	bFGF
R49042		16.17	-1.54	bFGF
R92031		6.32	1.33	bFGF
T57773		4.79	-2.27	VEGF

T81424	K-ALPHA-1	12.52	1.45	ENDOGRO
T87544		4.04	-1.40	ENDOGRO
T89094	RGS4	1156.70	1.71	ENDOGRO
U10991	G2	205.85	1.46	ENDOGRO
U17077	BENE	12.42	2.43	VEGF
U27655	RGS3	11.59	-2.23	bFGF
U27768	RGS4	102.15	1.68	ENDOGRO
U50534	13CDNA73	14.49	1.54	bFGF
U61166	ITSN1	4.45	-1.56	ENDOGRO
U79271	SDCCAG8	20.19	-1.33	ENDOGRO
U90908	LOC58504	7.01	1.30	ENDOGRO
W02693		5.01	-1.87	ENDOGRO
W44435	FLJ12649	6.30	-1.65	ENDOGRO
W46280		5.82	-1.65	ENDOGRO
W46364		630.21	-1.92	ENDOGRO
W60844		6.45	-1.30	ENDOGRO
W69778		32.69	-1.64	bFGF
W87772		472.27	1.26	VEGFE
X04706	HOXD4	38.81	1.55	ENDOGRO
X05610	COL4A2	83.40	-1.35	ENDOGRO
X66945	FGFR1	4.04	1.20	ENDOGRO
X68742	ITGA1	4.63	1.73	VEGF
X93921	DUSP7	6.85	1.34	ENDOGRO

Table. 4

RHMVEC Proliferation Signature

GenBank Accession Number	Gene Symbol	EC:MCF7 Intensity (Expression) Ratio	Fold Change	Growth Factor
600507553R1	600507553R1	6.40	-1.56	VEGF
600511339R1	600511339R1	10.95	-1.65	ENDOGRO
600513062R1	600513062R1	11.30	-1.84	VEGF
600516127R1	600516127R1	20.18	-1.97	VEGF
600516223R1	600516223R1	3.14	-1.25	bFGF
600518689R1	600518689R1	19.16	-1.92	VEGF
600523987R1	600523987R1	3.36	1.54	VEGF
600524312R1	600524312R1	9.60	-1.78	bFGF
700039220H1	700039220H1	3.64	1.31	bFGF
700067654H1	700067654H1	5.16	1.33	VEGF
700588837H1	700588837H1	3.28	-1.58	ENDOGRO
700690490H1	700690490H1	5.36	1.29	VEGF
701347738H1	701347738H1	4.31	-1.55	ENDOGRO
701349191H1	701349191H1	5.30	-1.50	bFGF
701350288H1	701350288H1	8.43	1.20	ENDOGRO
701353618H1	701353618H1	5.33	1.28	VEGF
701354577H1	701354577H1	5.05	1.49	VEGF
701354657H1	701354657H1	3.71	1.27	VEGF
701417958H1	701417958H1	3.13	1.20	bFGF
701419627H1	701419627H1	15.42	-1.76	ENDOGRO
AA799503	g2862458	4.90	-1.23	ENDOGRO
AA799750	Erg	482.85	-1.31	bFGF
AA800192	g2863147	4.60	-1.49	bFGF
AA800293	g2863248	104.39	-1.37	bFGF
AA800550	g2863505	39.16	1.20	VEGF
AA801220	g2864175	222.44	1.25	ENDOGRO
AA848714	g2936254	9.08	-1.26	bFGF
AA850055	g2937595	4.18	-1.26	bFGF
AA850311	g2937851	3.44	1.22	VEGF
AA851637	Lu	42.24	-1.51	ENDOGRO
AA859260	g2948611	3.32	-1.34	VEGF
AA859278	g2948629	4.10	1.36	bFGF
AA859444	g2947975	10.74	-1.73	bFGF
AA874964	g2979912	5.37	-1.33	VEGF
AA875261	g2980209	8.23	1.41	bFGF
AA891911	g3018790	9.75	1.35	bFGF
AA899923	g3035277	3.48	-1.44	bFGF
AA925057	g3072193	25.13	-1.36	VEGF

AA926129		74.21	-1.32	bFGF
AA944413	g3104329	3.96	1.21	VEGF
AA944542	g4132423	3.97	-1.23	bFGF
AA944936	g3104852	6.51	1.72	bFGF
AA945463	g3105379	3.61	-1.45	VEGF
AA945677	g3105593	29.07	-1.25	ENDOGRO
AA945788	g3105704	5.63	-1.20	VEGF
AA946190	g3106106	14.83	-1.28	VEGF
AA946201	g3106117	102.57	-1.25	ENDOGRO
AA946350	g3106266	80.11	1.45	bFGF
AA955134	g3513034	3.01	1.30	ENDOGRO
AA956085	g3119780	3.61	-1.23	bFGF
AA957335	g3121030	158.89	-1.55	bFGF
AA957776	g2936580	38.11	-1.18	bFGF
AA963106	g3136598	7.68	1.47	bFGF
AA964004	Pter	4.69	1.35	ENDOGRO
AA964264	g3137756	14.05	-1.20	bFGF
AA996897	g3187452	23.71	-1.24	ENDOGRO
AA997073	g3187934	5.63	-1.21	VEGF
AA998510	g3189161	26.21	-1.78	ENDOGRO
AA998516	g3189167	5.07	1.19	VEGF
AA998618	g3189269	3.48	-1.48	VEGF
AA999079	g3189670	3.67	-1.18	VEGF
AB000199	cca2	3.23	-1.31	VEGF
AB005540	PCTAIRE2	3.66	1.20	bFGF
AB010467	Abcc3	4.40	-1.28	VEGF
AB015308	Gna15	19.47	1.21	bFGF
AB015746	Il4r	22.40	-1.17	bFGF
AB019120	AB019120	67.88	-1.55	bFGF
AB020978	GADD45gamma	3.19	1.27	bFGF
AB032085	RM3	4.60	-1.28	bFGF
AB032087	g3730102	3.17	-1.18	ENDOGRO
AB060092	Scyb2	7.67	-1.76	ENDOGRO
AF003835	Idi1	3.42	1.32	ENDOGRO
AF021350	NKG2A	3.04	1.64	bFGF
AF029241	RT1.S3	5.62	-1.32	bFGF
AF047707	Ugcg	3.82	-1.65	VEGF
AF072816	mrp3	5.04	-1.30	bFGF
AF102262	beta1-4GT	3.91	-1.25	VEGF
AF154245	chemotactic protein-3	5.09	-1.32	bFGF
AF164039	AF164039	18.79	-1.31	bFGF
AF189709	collagen XVIII	14.86	-1.25	ENDOGRO
AF201901	interferon-gamma receptor	4.50	-1.50	bFGF
AF205717	LRTM4	8.60	1.20	VEGF
AF244366	FLIP short form	16.14	1.32	bFGF
AF254801	AF254801	69.37	1.29	bFGF

AF259504	Bak	4.27	-1.27	VEGF
AF259898	E3karp	10.92	-1.69	VEGF
AF271786	Fgf13	11.13	1.31	VEGF
AF314657	clusterin	10.00	-1.43	ENDOGRO
AF324255	Ero1l	3.40	-1.66	bFGF
AF368269	Cyp2t1	19.99	-1.38	ENDOGRO
AI008035	700068780H1	9.35	1.32	bFGF
AI008526	g3222358	16.48	2.48	bFGF
AI009368	g3223200	8.25	-1.34	VEGF
AI009736	g3223568	6.35	1.32	bFGF
AI009780	g3223612	3.02	1.23	bFGF
AI009783	g3223615	3.33	-1.32	ENDOGRO
AI010312	g4133226	31.15	-1.34	bFGF
AI011501	g3225333	17.92	-1.20	bFGF
AI012580	g3226412	10.77	-1.22	bFGF
AI012597	g3226429	13.23	1.19	bFGF
AI013470	g4133876	3.54	-1.48	ENDOGRO
AI013562	g3227618	7.03	-3.34	VEGF
AI029460	g3247286	5.84	-1.40	bFGF
AI031004	g3248830	80.92	-1.39	bFGF
AI043630	g3290365	13.96	1.23	bFGF
AI043724	g3290459	4.08	1.22	ENDOGRO
AI043851	g3290586	210.09	-1.35	bFGF
AI043958	g3290693	4.08	-1.20	VEGF
AI044026	g3290761	6.81	-1.34	bFGF
AI044530	g3291391	8.51	-2.18	bFGF
AI044674	g3291535	5.62	-1.49	VEGF
AI044760	g3291621	26.81	1.43	VEGF
AI044802	g3290865	4.52	-2.03	ENDOGRO
AI044912	g3291731	33.22	1.40	ENDOGRO
AI044948	g3291767	10.36	1.36	bFGF
AI045186	g3292005	21.40	-1.52	ENDOGRO
AI045920	g3292739	5.07	1.24	ENDOGRO
AI058759	g3332536	25.51	1.23	bFGF
AI059060	g3332837	3.24	-1.62	VEGF
AI059103	g3332880	14.45	-1.36	VEGF
AI059204	g3332981	55.91	-1.44	VEGF
AI059363	g3333140	124.38	1.40	bFGF
AI059449	g3333226	7.39	-1.34	bFGF
AI059450	g3333227	8.45	-1.69	VEGF
AI060115	g3333892	66.25	-1.25	VEGF
AI070068	g3396319	6.13	-2.29	bFGF
AI070370	g3396621	3.50	-1.23	ENDOGRO
AI072357	g3398551	7.13	1.22	ENDOGRO
AI101062	g3706050	4.44	-1.91	VEGF
AI101250	g4133997	4.27	1.45	bFGF
AI101270	g4134000	87.91	-1.28	bFGF

AI101402	g3706309	3.52	1.18	bFGF
AI101757	g3706619	6.05	-1.20	bFGF
AI101945	g3706786	6.82	-1.26	VEGF
AI102248	g4134070	13.24	-1.22	VEGF
AI102320	g3707114	3.90	-1.25	bFGF
AI103007	g3704802	3.47	-1.29	bFGF
AI103106	g3704827	3.90	1.47	bFGF
AI103618	g3708145	3.01	-1.36	VEGF
AI103939	g3704876	4.41	1.22	ENDOGRO
AI104128	g3708534	3.38	-1.36	VEGF
AI105417	g3709501	45.14	-1.30	VEGF
AI105452	g3709529	3.95	-1.44	VEGF
AI112636	g3512585	5.56	-1.25	bFGF
AI137629	g3638406	18.18	1.41	bFGF
AI137826	g3638603	3.28	-1.33	ENDOGRO
AI137944	g3638721	222.74	-1.76	bFGF
AI145002	g3666801	23.08	1.23	VEGF
AI145832	g3667631	6.35	-1.23	bFGF
AI168952	g3705260	5.36	1.21	VEGF
AI169422	g3705730	10.92	-1.37	VEGF
AI169635	g3709675	15.87	-1.21	ENDOGRO
AI171908	g3711948	3.49	-1.23	ENDOGRO
AI172056	g4134696	16.18	1.34	VEGF
AI172117	g4134703	10.06	-1.32	ENDOGRO
AI175466	g3726104	6.20	-1.45	bFGF
AI176486	g3727124	146.17	1.31	bFGF
AI176965	g4133497	82.43	-1.88	bFGF
AI176983	g3727621	3.19	1.26	bFGF
AI177055	g3727693	19.15	1.29	VEGF
AI177120	g3829605	4.30	-1.39	bFGF
AI177198	g3727836	4.37	1.16	VEGF
AI177396	g3728034	3.05	-1.62	bFGF
AI177621	g3728259	264.10	-1.28	bFGF
AI177939	g4135031	36.48	-1.32	VEGF
AI178222	g3728860	7.21	1.23	ENDOGRO
AI178718	g4135092	114.85	1.41	bFGF
AI178978	g3729616	7.39	-1.25	ENDOGRO
AI179786	g3730424	6.81	-1.33	VEGF
AI180386	g3731024	21.30	-1.50	VEGF
AI230758	g3814645	89.23	-1.24	ENDOGRO
AI230762	g3814649	3.23	-1.25	VEGF
AI230918	g3814805	3.00	-1.24	bFGF
AI231805	g3815685	43.95	-1.18	ENDOGRO
AI231999	g3815879	22.28	1.31	ENDOGRO
AI233099	g3816979	3.19	1.31	VEGF
AI233773	Mawbp	68.74	-1.27	bFGF
AI235721	g3829227	3.22	-1.32	VEGF

AI235960	g3829466	229.73	-1.23	VEGF
AI236381	g3829887	4.52	-2.09	bFGF
AI236799	g4136246	25.50	1.32	bFGF
AI236912	Nab1	7.23	1.24	bFGF
AI237544	g3831050	4.46	-1.28	bFGF
AI407547	g3727827	3.84	-1.17	bFGF
AI409186	g2938420	31.41	1.29	ENDOGRO
AI409841	g3706639	3.36	-1.26	VEGF
AI411054	g3812200	3.37	1.46	bFGF
AI711100	g3224246	385.26	-1.29	VEGF
AJ000696	KIF1D	4.52	-2.61	bFGF
AJ011116	nos3	58.27	-1.31	VEGF
AW140657	600510887R1	6.53	-1.44	ENDOGRO
AW142011	g3333577	3.20	-1.35	bFGF
AW142194	g2864225	41.07	1.23	VEGF
AW142519	g3071124	3.12	-1.39	bFGF
AW523549	g3224204	17.12	-1.22	bFGF
AW914004	g3224058	306.81	1.35	VEGF
AW916926	Slc22a7	13.17	-1.37	ENDOGRO
AW917188	Dpyd	9.05	1.63	VEGF
AW920825	701222534H1	32.82	1.57	VEGF
AY024364	GATA-3	4.64	-1.24	bFGF
BE098266	g3071239	323.96	-1.21	bFGF
BE108269	g3246659	6.26	1.34	ENDOGRO
BE121287	700032038H1	4.23	-1.16	ENDOGRO
BF283084	600520366R1	5.93	1.27	VEGF
BF398271	g3292264	7.25	-1.36	bFGF
BF416417	g3707631	4.83	-1.27	bFGF
BF548232	g3828538	3.62	-1.58	VEGF
BF551997	BF551997	21.20	1.33	bFGF
BG381698	g2672938	4.40	1.20	bFGF
BG664717	701222952H1	12.84	1.54	VEGF
BI275290	g3020546	3.50	-1.26	bFGF
BI277635	g3728852	9.73	-1.39	VEGF
BI283830	g3817681	9.65	-1.28	ENDOGRO
BI284263	g3137012	511.46	-1.25	bFGF
BI285246	g3830698	61.06	1.22	ENDOGRO
BI287221	g3705125	32.89	-1.24	VEGF
BI294910	g3705813	43.33	-1.51	ENDOGRO
BI296015	g3711886	5.26	-1.37	VEGF
BM384585	g2862699	6.07	-1.31	ENDOGRO
BM384701	g3224341	20.20	-1.42	VEGF
BM388598	g3187570	6.05	-1.56	bFGF
BM388852	g3106350	28.05	-1.19	bFGF
BM391182	600518660R1	4.10	-1.28	VEGF
BQ190671	g4132974	3.42	1.21	VEGF
BQ192029	g4133216	376.26	-1.31	bFGF

BQ198730	g3224083	39.70	1.24	VEGF
BQ199612	g3727571	29.44	-1.43	bFGF
BQ199678	g3818042	3.96	-1.35	bFGF
BQ200399	g3727330	128.03	1.21	bFGF
BQ203036	g2937343	10.46	1.20	VEGF
BQ203060	g3221834	19.92	-1.27	bFGF
BQ203246	g3102732	188.91	1.28	bFGF
BQ204980	g3222960	4.72	1.37	VEGF
BQ205927	g3103480	7.39	-1.25	bFGF
BQ779673	700052535F1	3.36	-1.43	bFGF
BQ780778	g2937314	29.44	-1.23	bFGF
BQ781420	g2936107	3.31	1.36	bFGF
BU671151		3.04	1.28	VEGF
BU671574	701216766H1	3.51	1.44	VEGF
CA333942	600524307R1	6.48	-1.57	VEGF
CA503512	g4134955	3.09	-1.30	VEGF
CA504040	g3709254	3.01	1.29	VEGF
CA506715	g2938431	102.56	1.24	bFGF
CA507008	g976837	3.86	-1.36	ENDOGRO
CA508330	g3813525	3.00	-1.25	VEGF
CA509105	600513095R1	3.10	-1.21	bFGF
CA509955	g3730145	37.61	1.42	bFGF
CA513003	701353736H1	3.92	1.23	bFGF
D00636	b5R	3.13	-1.26	bFGF
D11444	gro	3.41	-2.00	bFGF
D16339	g6981681	10.14	1.33	ENDOGRO
D16339	Ttpa	15.43	1.53	bFGF
D28860	D28860	3.78	-3.13	VEGF
D31838	wee1	4.16	1.34	VEGF
D42148	600520458R1	94.76	-1.47.	bFGF
D86086	Abcc2	5.88	1.21	bFGF
G2887744		9.40	-1.24	VEGF
G2887885		3.21	-1.58	ENDOGRO
G2888124		16.17	-1.70	ENDOGRO
G2937254		3.04	-1.36	bFGF
G2937336		3.11	-1.48	ENDOGRO
G2938797		6.83	1.24	bFGF
G2938805		3.65	-1.21	bFGF
G2938831		3.04	-1.33	bFGF
G2939578		6.47	-1.68	ENDOGRO
G3019428		39.84	1.20	VEGF
G3020059		7.27	-1.29	bFGF
G3021176		6.67	-1.33	bFGF
G3035644		5.53	1.32	bFGF
G3071714		3.04	-1.46	ENDOGRO
G3071902		167.52	-1.28	bFGF
G3072603		8.46	-1.26	bFGF

G3072712	56.89	1.22	ENDOGRO
G3073258	7.51	1.54	bFGF
G3102686	9.14	-1.38	bFGF
G3103279	34.67	1.38	ENDOGRO
G3137338	5.03	-1.53	VEGF
G3137782	22.69	1.33	VEGF
G3137957	273.68	-1.34	bFGF
G3137994	8.42	-1.34	bFGF
G3138006	6.05	-1.25	bFGF
G3189628	3.21	1.35	bFGF
G3224642	3.55	-1.69	VEGF
G3225906	14.76	1.21	bFGF
G3226018	5.47	-1.21	bFGF
G3226140	98.14	-1.31	bFGF
G3227787	13.27	-1.25	VEGF
G3246847	3.40	-1.48	bFGF
G3246942	135.33	-1.52	ENDOGRO
G3247784	14.84	-1.31	VEGF
G3247854	199.84	-1.30	bFGF
G3248097	26.74	1.35	bFGF
G3248367	21.02	-1.88	bFGF
G3291935	5.77	-1.46	ENDOGRO
G3291949	3.22	-1.16	VEGF
G3292531	18.79	-1.34	ENDOGRO
G3292629	3.80	-1.27	VEGF
G3333900	8.95	-1.34	ENDOGRO
G3333935	5.10	-1.21	bFGF
G3396358	3.87	-1.40	bFGF
G3396493	3.05	-1.32	VEGF
G3396557	26.97	-1.36	bFGF
G3396633	8.07	-1.45	bFGF
G3397437	304.78	-1.22	VEGF
G3397680	3.38	1.24	ENDOGRO
G3397969	9.69	-1.63	VEGF
G3398076	61.74	-1.60	bFGF
G3398171	4.81	-1.20	ENDOGRO
G3399145	22.81	-1.58	bFGF
G3399177	4.24	1.34	VEGF
G3399284	11.67	1.21	VEGF
G3399406	13.82	1.54	bFGF
G3511710	5.60	-1.27	VEGF
G3512937	31.87	-1.40	VEGF
G3513230	4.55	-1.21	bFGF
G3636910	5.68	1.20	VEGF
G3637432	14.94	-1.28	VEGF
G3637746	6.69	1.20	bFGF
G3638675	36.35	-1.27	VEGF

G3666728		3.09	-1.26	bFGF
G3666899		64.34	-1.48	bFGF
G3667173		8.07	-1.28	bFGF
G3707946		3.06	-1.27	bFGF
G3708389		17.55	-2.00	bFGF
G3708633		4.16	-1.35	VEGF
G3708986		95.05	-1.44	bFGF
G3709440		3.09	1.18	bFGF
G3710527		6.48	1.22	bFGF
G3710770		5.18	-1.19	bFGF
G3711240		8.06	-2.85	ENDOGRO
G3711421		22.68	-1.76	bFGF
G3711520		26.51	1.39	VEGF
G3711533		5.04	-1.39	bFGF
G3711566		31.85	1.34	ENDOGRO
G3712171		4.18	1.37	VEGF
G3725993		3.63	-1.22	ENDOGRO
G3726061		3.64	-1.16	ENDOGRO
G3727230		14.55	-1.37	VEGF
G3729898		1566.10	1.38	bFGF
G3730814		6.28	-2.55	bFGF
G3811611		6.82	-1.27	bFGF
G3812445		3.50	-1.28	bFGF
G3813207		398.22	-1.31	VEGF
G3813483		8.65	-1.50	ENDOGRO
G3829163		3.61	-1.32	bFGF
G4131670		3.34	1.24	VEGF
G4131679		5.44	-1.24	bFGF
G4131762		4.42	-1.46	ENDOGRO
G4132317		47.79	1.22	VEGF
G4132471		3.75	-1.22	bFGF
G915019		3.97	-1.30	VEGF
G976993		11.77	1.50	VEGF
G977252		3.56	-1.74	bFGF
G977371		9.43	-1.28	ENDOGRO
G977384		3.01	1.66	VEGF
G977468		3.82	-1.41	bFGF
G977854		5.07	-1.42	bFGF
G977919		5.12	-1.31	bFGF
G979053		10.84	-1.41	bFGF
H32317	g977734	3.08	1.32	VEGF
H32799	g978216	3.31	-1.65	VEGF
H34328	g979745	17.72	1.76	bFGF
H34385	g979802	7.34	-1.19	bFGF
H34603	g980020	4.26	1.43	VEGF
H34681	g980098	5.73	1.38	VEGF
J03637	AD mRNA	4.24	-2.80	bFGF

J03819	erb62	7.20	1.86	VEGF
L11995	cyclin B	3.64	1.22	VEGF
L20468	cerebroglycan	31.80	1.30	ENDOGRO
L22294	PDH	4.81	-1.47	ENDOGRO
L23128	L23128	3.23	1.20	bFGF
L27651	Slc22a7	7.71	-1.34	ENDOGRO
L34049	megalin	4.23	1.27	bFGF
M17412	LOC60380	4.02	-1.73	ENDOGRO
M26125	XEH mRNA	223.02	-1.53	ENDOGRO
M58040	transferrin receptor	3.87	1.28	bFGF
M80367	Gbp2	9.84	-1.62	bFGF
M81855	Abcb1	9.60	-1.79	bFGF
M83143	M83143	3.03	1.31	bFGF
M91235	M91235	11.54	-1.94	ENDOGRO
NM_012502	Ar	8.93	2.18	bFGF
NM_012528	Chrnb1	25.35	-1.31	bFGF
NM_012548	Edn1	392.42	-2.23	bFGF
NM_012566	Gfi1	14.50	1.39	bFGF
NM_012620	Serpine1	54.90	-2.51	ENDOGRO
NM_012679	Clu	3.34	-1.30	ENDOGRO
NM_012715	Adm	9.14	-1.97	ENDOGRO
NM_012762	Casp1	5.76	-1.26	bFGF
NM_012827	Bmp4	80.49	-1.44	bFGF
NM_012912	Atf3	4.89	-1.43	bFGF
NM_013000	Pam	7.26	1.40	bFGF
NM_013062	Kdr	405.26	1.34	bFGF
NM_013085	Plau	9.54	2.20	bFGF
NM_013130	Madh1	6.04	-1.20	ENDOGRO
NM_013145	Gnai1	14.79	1.48	bFGF
NM_013151	Plat	5.26	-1.38	ENDOGRO
NM_016987	Acly	3.21	-1.28	VEGF
NM_017028	Mx1	14.33	-1.79	bFGF
NM_017076	Tage4	10.54	1.78	bFGF
NM_017079	Cd1d	26.25	-1.30	bFGF
NM_017105	Bmp3	19.82	-2.20	ENDOGRO
NM_017112	Hpn	3.02	-1.91	VEGF
NM_017225	Pctp	5.87	1.30	bFGF
NM_017259	Btg2	26.14	-1.27	ENDOGRO
NM_017317	ram	4.89	-1.51	bFGF
NM_017350	Plaur	7.45	1.31	bFGF
NM_019144	Acp5	223.88	-1.54	ENDOGRO
NM_019147	Jag1	65.16	-1.46	VEGF
NM_019234	Dncic1	32.61	-1.51	bFGF
NM_019249	Ptprf	22.72	-1.20	ENDOGRO
NM_019261	Klrc2	11.07	1.78	bFGF
NM_019285	Adcy4	15.84	-1.18	bFGF
NM_019370	LOC54410	34.00	1.25	VEGF

NM_019371	SM-20	7.13	-1.61	ENDOGRO
NM_020072	Ppal	3.37	1.51	VEGF
NM_020082	Rnase4	25.93	1.41	VEGF
NM_021655	Chga	3.64	1.28	VEGF
NM_021679	Nxph3	6.16	1.28	ENDOGRO
NM_021751	LOC60357	140.84	-1.40	bFGF
NM_021846	Mcl1	8.92	1.36	VEGF
NM_022005	Fxyd6	812.43	-1.31	bFGF
NM_022177	Sdf1	9.97	-1.68	VEGF
NM_022224	Rpr1	3.40	1.38	bFGF
NM_022297	Ddah1	4.46	-1.28	VEGF
NM_022441	Acvrl1	61.21	-1.34	bFGF
NM_022528	Hif3a	3.50	-1.47	bFGF
NM_022705	Mch	12.79	-1.27	bFGF
NM_022715	Mvp	3.80	1.29	VEGF
NM_022856	Nab1	4.04	1.23	bFGF
NM_023103	Mug1	3.24	1.26	ENDOGRO
NM_023960	Kcnmb4	5.42	1.43	VEGF
NM_024160	Cyba	44.10	-1.34	bFGF
NM_030834	Mct3	27.50	-1.81	ENDOGRO
NM_030868	Nov	193.60	1.20	ENDOGRO
NM_030985	Agtr1a	33.27	2.02	VEGF
NM_031059	Msx1	4.48	-1.40	bFGF
NM_031100	Rpl10	4.31	-1.32	VEGF
NM_031242	Cds1	10.30	-1.37	bFGF
NM_031321	Slit3	5.51	-1.58	ENDOGRO
NM_031327	Cyr61	24.10	-1.65	ENDOGRO
NM_031544	Ampd3	24.58	-1.42	bFGF
NM_031550	Cdkn2a	7.80	1.40	bFGF
NM_031645	Ramp1	4.16	-1.47	ENDOGRO
NM_031646	Ramp2	14.25	-1.50	VEGF
NM_031771	Thbd	14.40	1.38	bFGF
NM_031807	Tpbg	66.41	-1.25	bFGF
NM_031970	Hspb1	52.18	-1.36	bFGF
NM_033237	Gal	546.73	-4.46	ENDOGRO
S68135	GLUT1	5.83	-1.52	ENDOGRO
S70011	g3137721	3.01	1.41	VEGF
S70011	tricarboxylate carrier	4.01	1.23	ENDOGRO
U03388	cyclooxygenase 1	22.47	-1.42	bFGF
U05989	Pawr	45.60	1.29	VEGF
U16858	testin	4.35	-1.47	ENDOGRO
U17604	rS-Rex-b	4.23	1.61	bFGF
U18060	PGHS-1	11.82	1.59	bFGF
U22830	P2Y purinoceptor	3.89	1.30	bFGF
U24174	WAF1	3.08	-1.32	ENDOGRO
U38376	Pla2g4a	10.63	1.23	bFGF
U39208	CYP4F6	8.18	-1.40	bFGF

U44948	SmLIM	33.23	1.19	VEGF
	chemokine receptor			
U54791	LCR1	20.18	1.41	ENDOGRO
U60085	CYP3A9	18.44	1.40	bFGF
U65656	gelatinase A	21.42	-1.33	bFGF
U72353	lamin B1	4.02	1.20	VEGF
U94330	OPG	3.13	-1.89	bFGF
U94709	EP4 prostanoid receptor	3.47	-2.55	VEGF
X00469	Cyp1a1	15.35	-2.04	bFGF
X00722	g3727098	3.04	-1.37	bFGF
X02601	Mmp3	8.70	1.55	bFGF
X13016	OX-45 mRNA	3.55	1.19	VEGF
X14264	CaMII	3.33	1.36	VEGF
X14977	Aldh2	3.11	-1.20	bFGF
X54862	Mgmt	23.74	-1.28	bFGF
X58830	vgr	22.26	-1.34	ENDOGRO
X63515	phosphorylase	3.93	-1.91	ENDOGRO
X63744	Slc1a3	7.36	-1.38	VEGF
X66539	TNF-alpha	3.97	-1.48	ENDOGRO
X68101	trg	4.28	1.19	VEGF
X70706	T-plastin	4.40	1.50	bFGF
X84004	cl100	20.03	-1.20	ENDOGRO
Y17328	CDK108	7.15	-1.45	bFGF
Z18877	Oas1	9.02	-3.11	bFGF

Table. 5

C6 Flank Tumor Model, Compound A-induced Signature, EC-specific Sequences

Compound-induced Fold Changes in Gene Expression

GenBank Accession Number	Gene Symbol	1 Dose	2 Doses	3 Doses
M10934	Rbp4	2.54	1.59	1.45
600519878R1	600519878R1	1.02	-1.94	-1.46
AA925717		1.09	1.34	1.62
AB028461	AB028461	1.36	2.08	1.51
AF056034	AF056034	-1.91	1.34	-2.03
AF058786	JE/MCP-1	1.47	1.58	1.38
AF058786	JE/MCP-1	1.44	1.62	1.36
AF154245	chemotactic protein-3	1.26	1.63	1.22
AF158385	ATP1B4	-2.03	1.40	-1.71
AF276998	Jam	1.07	-1.42	-1.84
AF295535	Ata3	-1.79	-1.30	-2.23
AJ299016	Ret	1.05	-1.65	-1.71
BF564460	BF564460	-1.08	-1.49	-1.78
D13871	glut 5 coding	-1.54	-1.65	-1.19
AA800146	g2863101	1.08	1.85	1.60
AA818658	g2888244	1.23	2.07	1.57
AA818845	g2888431	-2.40	1.13	-1.63
BG378083	g2888538	-1.80	1.42	-1.84
AA819832	g2889019	-1.26	-1.74	-1.75
AA848809	g2936349	1.28	1.85	1.59
G2937470	g2937470	-1.76	1.09	-2.73
BI282277	g2939494	-1.73	1.30	-1.66
BM390487	g2948168	-1.13	-1.81	-2.19
G3019978	g3019978	1.06	-1.39	-1.68
G3020570	g3020570	-1.01	-1.50	-1.65
AA900587	g3035941	-2.36	1.58	-2.63
AC091752	g3071324	1.22	1.79	1.46
G3073040	g3073040	1.02	-1.31	-1.69
G3103294	g3103294	-1.11	-1.70	-1.46
AA943790	g3103706	-2.49	1.33	-4.44
AA944827	g3104743	1.20	1.91	1.56
AA946094	Mb	-2.04	1.18	-2.31
AA946201	g3106117	1.47	2.25	1.31
AW251703	g3120965	1.20	1.73	1.51
G3136659	g3136659	-1.57	1.33	-1.70
G3136765	g3136765	-1.67	-1.54	-1.19
AA963444	g3137002	-1.68	-1.58	-1.27
AA996414	g3186969	1.01	-1.50	-1.66
AA996581	g3187136	-1.85	-1.23	-1.49
AI008203	g3222035	-1.72	-1.52	-1.32
CA503524	g3222465	1.24	1.95	1.60
AI009946	g3223778	-1.82	-1.59	-1.25
AI044213	g3291116	1.05	-1.44	-1.65
AI044263	g3291166	1.23	1.78	1.58

AI044643	g3291504	-1.01	-1.52	-1.66
AI059122	g3332899	1.14	1.70	1.26
BF558524	g3333166	-2.26	1.24	-2.52
AI059446	g3333223	-1.19	-1.77	-1.87
AI059511	g3333288	-1.66	-1.65	-1.30
G3398050	g3398050	-1.15	-2.01	-1.68
AI072733	g3398927	-1.47	1.16	-1.61
AI113026	g3512975	-1.19	-1.29	-1.71
G3637152	g3637152	-1.02	-1.36	-1.63
G3637289	g3637289	-1.02	-1.66	-1.96
AI137249	g3638026	-1.56	1.38	-1.78
AI137425	g3638202	-1.06	-1.91	-1.28
M31591	g3704673	1.44	2.24	1.90
G3708698	g3708698	-2.63	1.39	-2.88
AI104620	g3708949	-1.96	1.40	-1.71
AI105417	g3709501	-1.15	-1.85	-1.91
AI170840	g3710880	-2.23	1.43	-2.16
BQ211970	g3711814	-2.26	1.52	-2.37
G3725683	g3725683	-2.15	1.08	-3.22
CA503625	g3726615	-1.15	-1.66	-1.98
G3727000	g3727000	-1.19	-1.25	-1.64
AA924506	g3728041	1.17	-1.60	-1.35
AI178585	g3729223	1.03	-1.53	-1.77
G3811945	g3811945	1.15	1.89	1.53
G3813551	g3813551	1.10	-1.78	-1.47
AI231826	g3815706	-1.12	-1.72	-2.24
AI232784	g3816664	1.06	-1.36	-1.62
CA509598	g3817191	1.22	2.30	1.38
AI233962	g3817842	-1.81	1.19	-1.90
G977684	g977684	-1.61	-1.42	-1.20
K02111	MYHC mRNA	-1.70	-1.36	-1.50
L19998	Sult1a1	1.10	-1.80	-1.48
M11596	Calcb	1.03	1.41	1.59
M26125	XEH mRNA	1.06	-1.76	-1.48
M26744	IL6	1.37	1.71	1.02
M55534	alpha(B)-crystallin	1.04	1.65	1.41
M81785	syndecan	1.22	1.59	1.35
NM_012561	Fst	1.41	2.01	1.92
NM_012945	Dtr	1.27	1.95	1.28
NM_012949	Eno3	-2.30	1.36	-2.24
NM_013012	Prkg2	1.06	1.62	1.51
NM_013153	Has2	1.27	1.59	1.42
NM_017099	Kcnj8	1.06	-1.33	-1.63
NM_017117	Capn3	-2.03	1.43	-2.17
NM_017123	Areg	1.22	1.61	1.54
NM_017178	Bmp2	1.46	1.71	1.40
NM_017210	Dio3	1.21	3.37	1.69
NM_019156	Vtn	1.01	-1.53	-1.71
NM_019341	Rgs5	-1.11	-1.62	-2.01
NM_021588	Mb	-1.85	1.44	-1.99
NM_021666	Trdn	-1.55	1.43	-1.72
NM_022235	Kcne3	-1.58	-2.05	-2.07
NM_022604	Pg25	-1.66	-2.21	-2.73
NM_024483	Adra1d	1.25	1.61	1.29
NM_031327	Cyr61	1.13	1.65	1.29

NM_031345	Gilz	-1.29	-1.59	-1.60
NM_031970	Hspb1	-1.42	1.10	-1.77
U05341	p55CDC	-1.59	-1.42	-1.29
U23407	CRABP II	1.29	1.74	1.25
U53855	ratpgis	1.89	1.71	1.31
U94330	OPG	1.28	1.65	1.24
U94330	OPG	1.30	1.65	1.22
U94330	OPG	1.32	1.68	1.30
X15679	X15679	-1.37	-1.67	1.05
X52883	Sult1a1	1.11	-1.76	-1.54
Y13275	D6.1A protein	-1.24	-1.60	-2.50

**C6 Flank Tumor Model, Compound B-
induced Signature, EC-specific Sequences**

Compound-induced Fold Changes in
Gene Expression

GenBank Accession Number	Gene Symbol	1 Dose	2 Doses	3 Doses
600507547R1	600507547R1	1.33	2.22	1.53
AW140657	600510887R1	1.23	2.48	1.54
600522244R1	600522244R1	1.17	1.62	1.38
AI454872	700031879H1	-1.05	2.01	1.64
BQ206769	700064878H1	1.34	1.68	1.44
700510178H1	700510178H1	1.10	1.85	1.30
701216526H1	701216526H1	-1.04	-1.81	-1.43
AW920825	701222534H1	1.10	1.90	1.48
701347825H1	701347825H1	-1.70	-1.84	-1.99
701348620H1	701348620H1	-1.12	-1.62	-1.27
701350232H1	701350232H1	-1.10	-1.63	-1.23
AB005743	fatty acid transporter	1.35	1.87	1.45
AB011365	PPAR-gamma protein	1.16	1.83	1.36
AB011365	PPAR-gamma protein	1.17	1.95	1.45
AB032828	AB032828	-1.08	1.72	1.40
AB036792	ficolin-B	-1.77	-2.44	-2.34
AB060092	Scyb2	1.43	2.31	1.92
AF016387	RXRgamma	-1.09	-1.76	-1.41
AF058786	JE/MCP-1	1.18	1.78	1.61
AF058786	JE/MCP-1	1.22	1.78	1.56
AF081582	Kpl1	1.01	-1.81	-1.34
AF084934	RT1.D(u)	-1.39	-1.81	-1.41
AF087946	Gpr37	-1.07	-1.71	-1.36
AF131294	Abcd2	1.09	-1.65	-1.26
AF131294	Abcd2	1.06	-1.62	-1.25
AF146518	Enpep	1.15	2.35	1.75
AF154245	chemotactic protein-3	-1.05	1.78	1.45
AF314657	clusterin	-1.41	-1.61	-1.42
AW914760	AW914760	-1.23	-1.63	-1.42
AW914760	AW914760	-1.24	-1.60	-1.45
AW914760	AW914760	-1.23	-1.59	-1.36
AW920598	AW920598	1.21	1.61	1.50
D14839	rat FGF-9	1.10	1.74	1.66
D28560	NPH-type III	-1.20	-2.11	-1.37
D85509	MT3-MMP	-1.07	-2.11	-1.40
D89730	g2429082	1.21	4.18	1.82
BG381698	g2672938	1.01	1.66	1.42
AA799278	g2862233	-1.03	-1.89	-1.31
AA799657	g2862612	1.18	1.60	1.35
AA800145	g2863100	-1.03	1.68	1.30

AA800146	g2863101	1.20	1.75	1.49
BE115875	g2864040	1.12	1.67	1.40
G2888594	g2888594	1.07	2.38	1.65
G2888948	g2888948	-1.16	-1.62	-1.50
AA818607	g2889346	1.25	1.65	1.54
AA848639	g2936179	-1.20	2.23	1.52
AA848993	g2936533	1.39	1.70	1.46
AA849479	g2937019	-1.15	-1.68	-1.26
G2938081	g2938081	-1.06	1.67	1.29
G2939209	g2939209	1.17	1.82	1.41
AA858479	g2948819	1.12	-1.70	-1.28
AA875261	g2980209	1.08	1.67	1.37
BU758985	g3019743	1.02	1.76	1.26
G3019865	g3019865	-1.06	2.11	1.32
AA893022	g3019901	1.08	2.19	1.57
AA899521	g3034875	-1.26	-1.98	-1.41
AA925019	g3072155	-1.01	1.98	1.48
G3073258	g3073258	1.07	1.62	1.35
G3103279	g3103279	-1.15	2.14	1.61
AA943907	g3103823	-1.02	-1.62	-1.29
BQ204813	g3104100	1.16	2.06	1.45
BG375318	g3104739	-1.01	-1.79	-1.24
AA944827	g3104743	1.24	1.69	1.52
AA945643	g3105559	-1.92	-1.34	-1.71
G3105912	g3105912	1.10	2.31	1.38
AA946201	g3106117	1.11	2.01	1.41
AA946355	g3106271	-1.18	-1.61	-1.15
BQ201957	g3106396	-1.34	-1.99	-1.57
G3137782	g3137782	-1.06	1.77	1.33
G3137957	g3137957	-1.02	1.82	1.41
AA996727	g3187282	-1.41	-1.72	-1.63
BM391207	g3188195	-1.10	2.11	1.65
AA998510	g3189161	1.63	3.15	1.81
BQ202244	g3189311	-1.06	-1.83	-1.36
AA998953	g3189544	1.01	2.07	1.58
BQ203060	g3221834	-1.01	1.70	1.39
AI008526	g3222358	-1.04	1.70	1.33
CA503524	g3222465	1.18	2.02	1.38
AI009946	g3223778	1.03	-2.08	-1.39
BQ198730	g3224083	-1.00	1.76	1.37
AI010304	g3224136	1.23	1.72	1.40
AI502256	g3226632	-1.55	-2.23	-1.54
BI290624	g3227931	-1.06	-1.73	-1.35
AI029379	g3247205	1.17	1.64	1.31
G3247660	g3247660	-1.00	1.65	1.43
BQ196623	g3248862	1.43	2.17	1.43
AI411352	g3290939	-1.10	1.61	1.46
AI044052	g3290955	-1.32	-1.95	-1.44
AI044556	g3291417	1.04	2.21	1.51
AI044912	g3291731	1.06	1.89	1.53
AI044948	g3291767	1.29	1.80	1.29
AI045191	g3292010	1.01	3.41	1.60
G3292531	g3292531	1.12	2.03	1.65
AI058759	g3332536	1.35	1.80	1.54
AI103652	g3332682	1.22	1.91	1.36
AI059735	g3333512	-1.27	-1.47	-1.59

AF327511	Smhs1	1.06	1.66	1.35
BG377159	g3397026	1.03	1.71	1.22
BE099056	g3397110	1.02	1.61	1.31
G3397860	g3397860	1.13	1.64	1.42
AI072959	Mgll	1.00	2.03	1.37
G3512385	g3512385	-1.05	-1.85	-1.34
G3513248	g3513248	1.05	1.98	1.38
AI136855	g3637632	1.20	1.79	1.36
G3637836	g3637836	1.06	1.70	1.29
BI289488	g3638183	1.06	1.70	1.34
G3638417	g3638417	-1.30	-2.15	-1.25
G3638675	g3638675	1.27	2.08	1.53
G3638748	g3638748	1.18	1.67	1.36
G3666553	g3666553	-1.05	1.71	1.48
G3666899	g3666899	1.09	1.72	1.31
G3667679	g3667679	1.11	-2.68	-1.59
G3667962	g3667962	-1.12	-2.02	-1.45
G3668045	g3668045	1.24	1.63	1.34
M31591	g3704673	1.13	1.97	1.67
BI294910	g3705813	-1.04	1.83	1.36
AI101330	g3706248	-1.13	-1.66	-1.28
AI102081	g3706915	1.08	-1.76	-1.35
G3708538	g3708538	1.29	1.87	1.71
G3708830	g3708830	1.26	2.40	1.54
G3710429	g3710429	1.04	2.10	1.48
G3711566	g3711566	1.12	1.62	1.32
AI172274	g3712314	1.09	1.92	1.42
G3727230	g3727230	-1.09	1.63	1.35
G3727318	g3727318	1.14	1.79	1.38
AI176957	g3727595	-1.05	2.12	1.51
AI178367	g3729005	-1.12	-1.61	-1.49
AI179184	g3729822	-1.23	-1.96	-1.40
G3729898	g3729898	1.36	2.21	1.47
BE117878	g3730830	1.07	2.04	1.41
BF282318	g3730930	-1.90	-1.47	-2.02
G3811572	g3811572	1.07	2.42	1.58
BQ206905	g3812156	1.02	1.62	1.24
G3812233	g3812233	-1.13	-1.68	-1.23
G3813551	g3813551	1.50	1.87	1.28
BI283128	g3815073	1.16	1.93	1.45
NM_175582	g3816235	-1.45	-2.46	-1.96
AI232356	g3816236	1.16	1.77	1.34
AI232402	g3816282	1.07	1.70	1.25
CA509598	g3817191	1.10	1.68	1.25
AI407821	g3817623	-1.01	1.93	1.29
G3817759	g3817759	-1.08	-1.88	-1.35
G3828430	g3828430	1.01	1.99	1.40
G3828465	g3828465	1.16	2.40	1.71
BI278601	g3829380	-1.03	1.64	1.32
AI236212	g3829718	1.11	1.72	1.33
AI317824	g4033091	-1.37	-2.14	-1.88
AA800480	g4131501	1.35	2.36	1.41
G4132436	g4132436	-1.00	2.43	1.94
BQ192029	g4133216	-1.06	1.64	1.27
AI101250	g4133997	1.02	1.73	1.36
AI172271	g4134732	1.17	2.01	1.48

AI177939	g4135031	1.06	1.74	1.30
G807364	g807364	-1.15	1.63	1.28
H32476	g977893	-1.01	1.92	1.34
J03637	AD mRNA	-1.14	3.17	1.42
	platelet factor			
M15254	4	1.67	2.18	1.39
M18847	M18847	1.05	-1.68	-1.30
M23601	Maobf3	-1.06	1.74	1.32
	potassium			
M26161	channel	1.03	-1.96	-1.34
M26744	IL6	1.14	1.92	1.50
M81785	syndecan	1.06	1.72	1.32
NM_012561	Fst	1.10	1.84	1.65
NM_012733	Rbp1	-1.00	1.83	1.54
NM_012771	Lyz	-1.49	-1.53	-1.69
NM_012908	Tnfsf6	1.04	-1.64	-1.39
NM_012908	Tnfsf6	1.02	-1.61	-1.39
NM_013012	Prkg2	1.31	2.03	1.48
NM_013057	F3	1.06	1.65	1.46
NM_013080	Ptprz1	-1.11	-1.61	-1.30
NM_013191	S100b	1.04	-1.86	-1.37
NM_016994	C3	-1.74	-1.94	-2.10
NM_017061	Lox	-1.22	2.17	1.63
NM_017083	Myo5b	1.82	3.00	1.62
NM_017161	Adora2b	1.07	2.13	1.45
NM_017173	Serpinh1	1.03	1.83	1.32
NM_017210	Dio3	1.97	1.69	2.45
NM_017354	RNU16845	1.05	-2.04	-1.33
NM_019343	Rgs7	1.09	1.87	1.43
NM_019355	CPG2	-1.22	-2.12	-1.24
NM_019358	Gp38	1.05	1.94	1.25
NM_019370	LOC54410	1.02	2.31	1.70
NM_020082	Rnase4	-1.03	1.86	1.43
NM_020542	LOC57301	1.22	1.64	1.39
NM_021698	F13a	1.21	1.64	1.31
NM_022182	Fgf7	1.00	1.79	1.41
NM_022226	Prsc1	1.03	1.65	1.24
NM_022230	Stc2	1.07	1.59	1.45
NM_022236	Pde10a	-1.02	1.59	1.17
NM_022849	Crpd	-1.07	1.70	1.39
NM_022925	Ptprq	1.29	1.71	1.13
NM_024142	LOC79110	-1.06	-1.60	-1.49
NM_024159	Dab2	1.03	1.82	1.29
NM_030656	Agxt	1.18	1.61	1.24
NM_030832	Fabp7	1.17	2.32	1.70
NM_030990	Plp1	-1.05	-2.33	-1.53
NM_031012	Anpep	-1.14	1.67	1.35
NM_031022	Cspg4	-1.14	-1.70	-1.23
NM_031050	Lum	-1.17	1.97	1.52
NM_031334	Cdh1	-1.32	-2.12	-1.39
NM_031645	Ramp1	1.07	1.63	1.21
NM_031712	Pdzk1	-1.43	-1.86	-1.62
NM_031713	Pirb	-1.68	-1.37	-1.59
NM_031716	Wisp1	-1.03	1.88	1.43
NM_031736	Slc27a2	-1.07	-1.72	-1.71
NM_031761	Figf	-1.03	1.84	1.39

NM_031807	Tpbg	1.04	1.77	1.44
NM_032060	C3ar1	1.20	1.68	1.29
S72505	glutathione S-transferase Yc1 subunit	1.72	2.68	1.39
S72505	glutathione S-transferase Yc1 subunit	2.01	2.79	1.50
S72505	glutathione S-transferase Yc1 subunit	2.02	2.92	1.65
S82820	GSTA5	1.91	2.60	1.46
U04808	Rbs11	-1.18	-1.61	-1.33
U36992	cytochrome P450 Cyp7b1	-1.22	1.78	1.49
U36992	cytochrome P450 Cyp7b1	-1.20	1.82	1.57
U36992	cytochrome P450 Cyp7b1	-1.22	1.84	1.63
U39943	CYP2J3	-1.12	-1.72	-1.40
U53855	ratpgis	1.33	2.53	1.59
U57062	RNKP-4	-2.10	-1.70	-2.07
U65217	U65217	-1.50	-2.21	-1.55
U65656	gelatinase A	-1.01	2.05	1.43
U66470	U66470	1.16	2.05	1.41
U75581	A-FABP	1.55	2.22	1.69
U75581	A-FABP	1.60	2.46	1.73
U75581	A-FABP	1.60	2.48	1.79
U81037	NrCAM	1.24	2.20	1.43
U85512	Gchfr	1.41	1.74	1.64
U94330	OPG	1.01	1.66	1.34
X15679	X15679	1.07	-2.00	-1.33
X59859	DCN	-1.02	2.43	1.60
X68312	IgM	-1.19	-2.16	-1.50
X78997	cadherin	-1.21	-1.79	-1.35
Z30663	Z30663	1.06	-1.74	-1.36

MatBlll Tumor Model, Compound A-induced Signature, EC-specific Sequences

GenBank Accession Number	Gene Symbol	Compound-induced Fold Change in Gene Expression
600511261R1	600511261R1	1.61
600512030R1	600512030R1	-2.01
600516277R1	600516277R1	1.70
600521787R1	600521787R1	2.45
600521928R1	600521928R1	-1.72
600522339R1	600522339R1	1.72
700031150H1	Hbb	-2.93
700031292H1	Hbb	-2.95
700033761H1	700033761H1	-1.69
700035711H1	700035711H1	-1.77
700036014H1	Hbb	-3.21
700037874H1	700037874H1	-2.14
700040546H1	700040546H1	-2.36
700041049H1	700041049H1	-2.47
700509540H1	700509540H1	1.59
701217088H1	701217088H1	1.80
701347811H1	701347811H1	-1.74
AA012768	g1473830	1.72
AA799471	g2862426	3.28
AA799964	g2862919	1.62
AA800145	g2863100	-1.75
AA800690	700036377H1	-3.01
AA800790	g2863745	-2.53
AA801013	g2863968	2.88
AA818163	g2888043	1.78
AA818207	700035764H1	-3.04
AA818804	g2888390	1.81
AA818845	g2888431	2.74
AA819500		-1.68
AA848265	g2935805	1.88
AA848809	g2936349	1.60
AA858479	g2948819	1.65
AA859373	g2948724	2.23
AA874889	g2979837	-2.20
AA874924	g2979872	-1.69
AA892298	g3019177	-1.61
AA900587	g3035941	1.99
AA924082	g3071218	1.59
AA943742	g3103658	-1.76
AA943743	g3103659	-2.53
AA944410	g3104326	-1.74
AA945100	g3105016	-1.60

AA945119	Hbb	-3.64
AA945677	g3105593	1.95
AA945951	g4132652	5.93
AA946094	Mb	2.83
AA946457	g4132801	-2.19
AA956834	g3120529	-2.23
AA963068	g3136560	-2.08
AA963366	g3136858	2.43
AA996698	g3187253	-1.67
AA997375	g3187690	1.71
AB011533	MEGF7	-1.70
AC091752	g3071324	1.78
AF009329	SHARP-1	1.83
AF015304	Slc29a1	1.69
AF037272	ps20	1.75
AF055286	3-Oct	1.80
AF056034	AF056034	2.30
AF058786	JE/MCP-1	-1.80
AF058786	JE/MCP-1	-1.76
AF058786	JE/MCP-1	-1.69
AF063102	CIRL-2	-1.80
AF109393	podocalyxin	-2.34
AF109674	Lgl1	1.61
AF134409	Rhes protein	2.29
AF146518	Enpep	-2.03
AF150082	DDP1	-1.66
AF157005	MYHC	6.94
AF158385	ATP1B4	2.57
AF159103	Tnfip6	-1.67
AF160978	C1qRp	-2.02
AF173834	calpain isoform Rt88'	1.96
AF269251	mob-5	1.97
AF271786	Fgf13	2.06
AF314657	clusterin	2.13
AF323174	Clic5	2.57
AF364071	Smpx	2.64
AF372834	g4135229	1.63
AF404762	g3704880	1.67
AF450248	Actn3	3.96
AI008526	g3222358	-2.88
AI009020	600518256R1	1.61
AI009669	g3223501	-1.61
AI011757	g3225589	-1.62
AI013912	g3227968	-1.72
AI029383	g3247209	3.23
AI030556	g3248382	1.77
AI043880	g3290615	1.76

AI044257	g3291160	1.99
AI044658	g3291519	2.38
AI044948	g3291767	-1.94
AI045276	g3292095	-2.89
AI058243	700034477H1	-1.69
AI059662	g3333439	1.98
AI070419	g3396670	-1.65
AI071230	g3397445	1.80
AI071570	600520320R1	2.07
AI072669	g3398863	1.78
AI072687	g3398881	1.64
AI072733	g3398927	1.68
AI072751	g3398945	-1.70
AI102560	g3707304	-2.36
AI104898	g3708043	2.57
AI104955	g3709178	2.22
AI113026	g3512975	-2.36
AI137425	g3638202	-2.48
AI137674	g3638451	1.79
AI144943	g3666742	1.87
AI169239	g3705547	-3.08
AI169311	g3705619	1.78
AI170840	g3710880	2.19
AI170948	g3710988	-1.77
AI171466	g3711506	1.87
AI172271	g4134732	-2.04
AI175988	g3726626	3.28
AI176957	g3727595	-2.20
AI177013	g3727651	1.65
AI177057	g4134951	-3.44
AI177392	g3728030	-1.67
AI177951	g3728589	-1.82
AI178376	g4135065	1.60
AI178585	g3729223	-2.30
AI178996	g3729634	1.59
AI231053	g3814933	-1.91
AI231438	g3815318	1.61
AI233773	Mawbp	1.77
AI235210	g4136063	-4.17
AI235960	g3829466	-1.66
AI236229	g4136175	3.67
AI409186	g2938420	-2.62
AI411737	Hbb	-3.37
AI412460	g3704629	-1.65
AI603145	g3707784	2.62
AJ242926	irl685	2.05
AJ426426	600524449R1	1.68

AW253240	700039226H1	-3.10
AW915763	600523193R1	1.65
AW916287	g2980074	-1.71
AY027527	NADPH oxidase 4	-1.66
AY115564	g3712131	2.68
BE109616	g2862726	2.56
BE117010	g2949577	-2.03
BF287821	700065626H1	-1.63
BF393825	g3814029	-1.59
BF395396	g3187656	2.88
BF401710	g2863152	1.63
BF419896	600508357R1	-1.67
BF558524	g3333166	1.94
BG373503	g3138384	-1.65
BG374556	700510594H1	1.61
BG378083	g2888538	2.54
BG670348	g3332207	-1.62
BI274062	Trela	2.08
BI277462	g3729596	-1.96
BI279373	g3814946	1.70
BI282277	g2939494	2.23
BI283128	g3815073	-2.27
BI285246	g3830698	-1.81
BI291451	g2889589	-1.78
BI294910	g3705813	-1.88
BI296277	g3705123	-1.67
BM386121	g2862284	-2.23
BM390441	g3707901	-1.67
BQ190196	g3831151	-1.78
BQ191387	g3512957	1.72
BQ194973	g3118966	-1.93
BQ196248	g2938644	-1.65
BQ199466	g3712138	-1.67
BQ199747	g3707262	-1.65
BQ204163	g3291004	4.70
BQ206937	g3816206	1.59
BQ208795	LOC85383	1.75
BQ211970	g3711814	1.84
BQ779790	g3709350	2.08
BU758944	g3729204	-1.62
CA503430	g3818031	-2.01
CA503625	g3726615	-1.97
CA505509	g3020114	2.75
CA507161	g3226571	-1.77
CA508003	g3707933	-1.89
CA509083	g3397522	1.59
CA509145	g3727217	1.93

CA509211	g3704741	-1.60
CA509598	g3817191	2.15
CA509955	g3730145	-1.74
D12520	nitric oxide synthase	1.63
D14051	nitric oxide synthase	1.62
D28561	glucose transporter	2.60
D63164	cyclin E	-1.66
D86800	D86800	-1.92
D86800	D86800	-1.85
G2863860		3.31
G2889725		2.55
G2939329		-1.67
G3018718		-1.64
G3018906		-2.03
G3020570		-1.63
G3036209		-1.61
G3072525		3.27
G3072678		2.28
G3073004		-1.77
G3105912		-1.63
G3136659		2.50
G3138335		-2.07
G3187018		-1.69
G3225225		-1.92
G3226067		-2.21
G3226140		5.03
G3226701		2.48
G3227787		-2.28
G3291802		-1.77
G3292543		2.04
G3396388		1.91
G3396690		-1.99
G3396723		1.77
G3397083		1.59
G3397437		-1.72
G3397917		-1.62
G3397969		-2.39
G3398441		-2.39
G3399406		-2.47
G3513002		1.96
G3513248		-2.52
G3636896		-1.94
G3637290		1.97
G3637649		1.60
G3637836		1.69
G3638063		-1.64
G3638106		-1.60

G3638248		-1.86
G3666834		-1.75
G3667558		-1.64
G3667798		-1.59
G3708538		-1.59
G3708698		3.29
G3708830		1.72
G3708934		1.61
G3709332		1.78
G3709581		-1.76
G3710109		-1.87
G3710353		-1.89
G3710419		-1.60
G3710427		-1.67
G3710782		1.72
G3712041		-1.70
G3712094		3.52
G3712205		1.79
G3712229		1.68
G3725978		3.71
G3726013		2.02
G3726093		1.91
G3726475		-3.16
G3727000		1.91
G3727318		-1.61
G3811492		-2.18
G3812333		-1.88
G3813207		-1.60
G3817985		-1.66
G4131487		1.95
G4131762		1.84
G4135671		2.78
G977371		1.70
G978154		-1.86
H35065	g980482	3.04
J02582	apoE	1.64
J02585	s-CoA d mRNA	2.04
K00781	g3247405	1.94
L00381	L00381	2.50
L16764	HSP70	1.60
L16764	HSP70	1.70
L16764	HSP70	1.79
L20681	Ets-1	-1.59
M11670	cat mRNA	1.60
M11851	MLC2 mRNA	2.69
M26744	IL6	-2.45
M26744	IL6	-2.38

M26744	IL6	-2.35
M29853	P-450 mRNA	2.02
M29853	P-450 mRNA	2.03
M34097		-1.64
M55149	pap	2.08
M58040	transferrin receptor	-1.81
M60616	UMRCase	1.81
NM_012491	Add2	-1.78
NM_012497	Aldoc	1.60
NM_012505	Atp1a2	3.08
NM_012530	Ckm	2.64
NM_012588	Igfbp3	-3.62
NM_012604	Myh3	2.35
NM_012605	Myl2	2.36
NM_012771	Lyz	-1.74
NM_012786	Cox8h	3.99
NM_012812	Cox6a2	2.55
NM_012864	Mmp7	2.08
NM_012949	Eno3	3.06
NM_012966	Hspe1	-1.71
NM_013037	Il1rl1	-1.79
NM_013044	Tmod	2.36
NM_013062	Kdr	-3.79
NM_013153	Has2	-1.82
NM_013186	Kcnb1	2.96
NM_013197	Alas2	-2.48
NM_017049	Slc4a3	1.67
NM_017066	Ptn	-1.97
NM_017104	Csf3	1.85
NM_017115	Myog	2.53
NM_017117	Capn3	2.47
NM_017131	Casq2	1.66
NM_017184	Tnni1	1.96
NM_017185	Tnni2	3.43
NM_017328	Pgam2	3.97
NM_017333	Etb	-2.74
NM_019131	Tpm1	1.97
NM_019212	Acta1	3.55
NM_019278	Resp18	1.69
NM_019282	Cktsf1b1	-1.82
NM_019292	Ca3	2.82
NM_019334	Pitx2	2.84
NM_019341	Rgs5	-1.83
NM_021588	Mb	2.44
NM_021593	Kmo	-1.62
NM_021666	Trdn	1.64
NM_021693	LOC59329	1.61

NM_022235	Kcne3	-11.33
NM_022396	Gng11	-1.80
NM_022604	Pg25	-6.48
NM_022631	Wnt5a	-1.74
NM_022674	H2afz	-1.74
NM_023991	Prkaa2	3.17
NM_024141	Thox2	2.32
NM_030856	Lrrn3	-1.87
NM_031007	Adcy2	1.94
NM_031022	Cspg4	-1.77
NM_031039	Gpt	1.70
NM_031511	Igf2	3.83
NM_031531	Spin2c	2.18
NM_031612	Apel	-2.36
NM_031715	Pfkm	1.68
NM_031813	Mybph	1.84
NM_032063	Dll1	-1.76
NM_032072	Appbp1	-1.71
U22520	IP-10	-2.40
U25281	CR16	1.60
U25684	U25684	-1.60
U31935	CAP2	2.53
U94330	OPG	-1.68
X67654	glutathione transferase	1.69
X81449	g587519	1.68
X82152	fibromodulin,unnamed	1.92
X92069	P2X5	1.86
X98517	Mmp12	1.66

Table. 6

C6 Flank Tumor Model, Compound A

GenBank Accession Number	Gene Symbol
600520186R1	
701217994H1	
AA945677	g3105593
AA957449	g3121144
AA964264	g3137756
AB015308	Gna15
AF154245	chemotactic protein-3
AF244366	FLIP short form
AF314657	clusterin
AI010322	g3224154
AI012597	g3226429
AI059363	g3333140
AI136847	g3637624
AI236799	g4136246
AI454865	g3103424
AW142194	g2864225
BI285246	g3830698
BQ207019	g3730060
G2938456	
G2938797	
G3021176	
G3137780	
G3138247	
G3225906	
G3396115	
H32810	g978227
H34187	g979604
L20468	cerebroglycan
NM_012922	Casp3
NM_013085	Plau
NM_017105	Bmp3
NM_031327	Cyr61
NM_080783	600519254R1
U17604	rS-Rex-b
U18060	PGHS-1
Y15685	g2648067

C6 Flank Tumor Model, Compound B

GenBank Accession Number	Gene Symbol
600520186R1	
700510178H1	
701217994H1	
701419627H1	
AA964264	g3137756
AB015308	Gna15
AF075704	Ata1
AF140232	S100A6
AF154245	chemotactic protein-3
AI008035	700068780H1
AI009736	g3223568
AI010322	g3224154
AI012085	g4133563
AI012597	g3226429
AI059363	g3333140
AI136847	g3637624
AI177939	g4135031
AI228076	g4135309
AI454865	g3103424
AW140657	600510887R1
BE115875	g2864040
BI278601	g3829380
BI285246	g3830698
BI294910	g3705813
BQ192029	g4133216
BQ196623	g3248862
BQ203060	g3221834
D89730	g2429082
G2938081	
G2946933	
G3072603	
G3137780	
G3137957	
G3138247	
G3292531	
G3396115	
G3397675	
G3512937	
G3638675	
G3666553	
G3666899	
G3710770	
G3726475	
G3813551	

G3814512
G977854
M81855   Abcb1
NM_012566   Gfi1
NM_019261   Klrc2
NM_022925   Ptprq
NM_031518   Mox2
NM_080783   600519254R1
U36992   cytochrome P450 Cyp7b1
U60085   CYP3A9
U60085   CYP3A9
U65656   gelatinase A
Y15685   g2648067

MatBlll Tumor Model, Compound A

GenBank Accession Number	Gene Symbol
600520186R1	
701219674H1	
AA800293	g2863248
AA848602	g2936142
AA859467	g2948987
AA945677	g3105593
AA957449	g3121144
AA963106	g3136598
AA996897	g3187452
AF022774	Rph3al
AF248543	iGb3 synthase
AF314657	clusterin
AF368269	Cyp2t1
AI008526	g3222358
AI010322	g3224154
AI012085	g4133563
AI012597	g3226429
AI044404	g3291307
AI044948	g3291767
AI045276	g3292095
AI169311	g3705619
AI170948	g3710988
AI176957	g3727595
AI228076	g4135309
AI233773	Mawbp
AI409186	g2938420
AI454865	g3103424
AW142194	g2864225
BI278601	g3829380
BI285246	g3830698
BM388852	g3106350
BM390441	g3707901
BQ196557	g3729556
D16339	g6981681
D16339	Ttpa
D88666	PS-PLA1
G2938797	
G3034536	
G3226140	
G3396115	
G3398076	
G3399406	
G3513248	

G3638802
G3666553
G3666899
G3667173
G3711240
G3725764
G3730626
G3813079
G977371
H32810   g978227
H35065   g980482
NM_012715   Adm
NM_013062   Kdr
NM_021676   Shank3
NM_021751   LOC60357
NM_022242   Niban
NM_022959   P-cip1
NM_031327   Cyr61
NM_031544   Ampd3
NM_031658   Msln
U03388   cyclooxygenase 1
U18771   Rab26
U38419   LOC64305
X63515   phosphorylase

EXAMPLE 6   BIOMARKER VALIDATION

        In order to confirm that the seven genes we identified as potential biomarkers of tumor endothelial cell proliferation were specifically expressed in tumor vasculature and whose expression levels reflected endothelial cell proliferation rates, we performed several validation experiments. First,

5   we independently assessed gene expression levels in the animal tumor RNA samples by quantitative realtime PCR to confirm the microarray hybridization results. The biomarker data obtained from the microarray experiments described above was validated by real time quantitative real time PCR. Results: Quantitative real time PCR was performed with gene-specific PCR primer pairs and amplicon-specific fluorescent probes (TaqMan). For each RNA sample tested, transcript abundance of GAPDH

10   was determined. In addition, transcript abundance of genes of interest and GAPDH were determined for a calibrator RNA sample (total rat lung RNA). (A) Fold changes in gene expression in tumors from KDR kinase-treated animals relative tumors from vehicle-treated animals were calculated using the $\Delta\Delta CT$ method (see Materials and Methods). mRNA levels for each gene in the rat tumors are also shown relative the calibrator RNA pool (B). As shown in Figure 7, the results obtained from the real time PCR

15   studies closely matched those from the DNA microarrays (Figure 7).

        We also measured the expression levels of the biomarker genes in an additional set of rat MatBIII tumors from a fourth animal study for which no gene expression profiling was performed. In this independent study, animals with established MatBIII breast tumors (seven days post cell implantation) were dosed orally once per day with Compound A or vehicle for a total of eight days.

20   Half of each tumor from our animal tumor studies was fixed and preserved for sectioning and immunohistochemistry as described in Materials and Methods. In order to determine if expression of the biomarker genes was specific to the endothelial cells within tumors, we visualized their protein products in rat tumor tissue sections by immunofluorescence microscopy. Antibodies are available commercially for five of the seven biomarker protein products and we were able determine optimal conditions for

25   immunofluorescence staining. Individual tumor sections approximately 3-5 um thick were de-waxed, rehydrated and incubated with antibodies against one of the biomarker proteins and also with antibodies against the endothelial cell surface protein CD31 (to label the tumor vasculature). De-waxed, re-hydrated MatBIII tumor sections were incubated with antibodies against CD31 and one of the following biomarker proteins: CLU, ANGPT2, CYR61, ENDRB, or PLAU. Primary antibodies bound to the biomarker

30   proteins and CD31 were visualized with Alexa488-labeled and Alexa546-labeled secondary antibodies, respectively as described in Materials and Methods. After mounting under coverslips, images were captured with a Zeiss Axiocam through a Zeiss Axiovert 135 fluorescence microscope equipped with a 40x objective.

        Results: We found that the five proteins we examined (ANGPT2, CLU, CYR61, EDNRB, and PLAU)

35   were each localized specifically to the tumor vasculature in MatBIII tumors (Figure 8). Indicating that

biomarker protein expression in rat mammary tumors is localized to vasculature. The expression levels of all genes with the exception of Cyr61 changed as expected in response to exposure to the KDR kinase inhibitor.

Finally, we correlated the confirmed expression changes of the biomarker genes in Compound A-treated tumors with an independent measure of tumor endothelial cell proliferation. Using a modification of the method described by Mundhenke, et al. (Mundhenke, 2001), we measured endothelial cell proliferation rates by double immunohistochemical staining of tumor sections for the endothelial cell marker CD31 and the nuclear proliferation marker Ki67. We analyzed C6 flank tumors from five vehicle-treated animals and five Compound A-treated animals (3 doses vehicle or compound over 72 hrs).

Results: We determined the endothelial cell proliferation rate in tumors from vehicle treated animals to be 34% +/- 5%. In contrast, we determined that the endothelial cell proliferation rate was only 19 % +/- 5% in tumors from animals treated with Compound A.

While the present invention has been described with reference to what are considered to be the specific embodiments, it is to be understood that the invention is not limited to such embodiments. To the contrary, the invention is intended to cover various modifications and equivalents included within the spirit and scope of the appended claims. For example, while the disclosure focuses on using the disclosed biomarkers for detecting the efficacy of a KDR kinase inhibitor, the use of similar methods to evaluate the ability of other cancer therapeutics to regulate the proliferative state of vascular endothelial cells within tumors are specifically within the scope herein.

All references cited throughout the disclosure are hereby expressly incorporated by reference.

References Cited in the Specification

1.   N. Ferrara, H. Heinsohn, C. E. Walder, S. Bunting, G. R. Thomas, Ann N Y Acad Sci 752, 246-56 (Mar 27, 1995).

2.   N. Ferrara, H. P. Gerber, J. LeCouter, Nat Med 9, 669-76 (Jun, 2003).

3.   D. W. Leung, G. Cachianes, W. J. Kuang, D. V. Goeddel, N. Ferrara, Science 246, 1306-9 (Dec 8, 1989).

4.   N. Ferrara, Nat Rev Cancer 2, 795-803 (Oct, 2002).

5.   K. J. Kim et al., Nature 362, 841-4 (Apr 29, 1993).

6.   T. P. Quinn, K. G. Peters, C. De Vries, N. Ferrara, L. T. Williams, Proc Natl Acad Sci U S A 90, 7533-7 (Aug 15, 1993).

7.   R. L. Kendall et al., J Biol Chem 274, 6453-60 (Mar 5, 1999).

8.   H. P. Gerber, N. Ferrara, J Mol Med 81, 20-31 (Jan, 2003).

9.   N. Ferrara, Semin Oncol 29, 10-4 (Dec, 2002).

10.   H. Gille et al., J Biol Chem 276, 3222-30 (Feb 2, 2001).

11.   C. Mundhenke et al., Clin Cancer Res 7, 3366-74 (Nov, 2001).

12.   M. E. Fraley et al., Bioorg Med Chem Lett 12, 3537-41 (Dec 16, 2002).

13.   P. J. Manley et al., Bioorg Med Chem Lett 13, 1673-7 (May 19, 2003).

14.   M. T. Bilodeau et al., Bioorg Med Chem Lett 13, 2485-8 (Aug 4, 2003).

15.   M. E. Fraley et al., Bioorg Med Chem Lett 13, 2973-6 (Sep 15, 2003).

16.   T. R. Hughes et al., Nat Biotechnol 19, 342-7 (Apr, 2001).

17.   M. J. Marton et al., Nat Med 4, 1293-301 (Nov, 1998).

18.   H. M. DeLisser, P. J. Newman, S. M. Albelda, Curr Top Microbiol Immunol 184, 37-45 (1993).

19.   B. R. DeYoung et al., J Cutan Pathol 22, 215-22 (Jun, 1995).

20.   H. M. DeLisser, P. J. Newman, S. M. Albelda, Immunol Today 15, 490-5 (Oct, 1994).

21.   D. C. Brown, K. C. Gatter, Histopathology 40, 2-11 (Jan, 2002).

22.   D. C. Brown, K. C. Gatter, Histopathology 17, 489-503 (Dec, 1990).

23.   B. A. Keyt et al., J Biol Chem 271, 5638-46 (Mar 8, 1996).

24.   C. de Vries et al., Science 255, 989-91 (Feb 21, 1992).

25.   J. Lauren, Y. Gunji, K. Alitalo, Am J Pathol 153, 1333-9 (Nov, 1998).

26.   L. Zhang et al., Cancer Res 63, 3403-12 (Jun 15, 2003).

27.   P. J. Svensson, M. Anvret, M. L. Molander, A. Nordenskjold, Hum Genet 103, 145-8 (Aug, 1998).

28.   K. Kikuchi et al., Biochem Biophys Res Commun 219, 734-9 (Feb 27, 1996).

29.   M. Okada, M. Nishikibe, Cardiovasc Drug Rev 20, 53-66 (Winter, 2002).

30.   R. Lahav, G. Heffner, P. H. Patterson, Proc Natl Acad Sci U S A 96, 11496-500 (Sep 28, 1999).

31.   D. A. Withers, S. I. Hakomori, J Biol Chem 275, 40588-93 (Dec 22, 2000).

32.   A. Taniguchi, R. Suga, K. Matsumoto, Biochem Biophys Res Commun 273, 370-6 (Jun 24, 2000).

33.   I. P. Trougakos, E. S. Gonos, Int J Biochem Cell Biol 34, 1430-48 (Nov, 2002).

34.   S. E. Jones, C. Jomary, Int J Biochem Cell Biol 34, 427-31 (May, 2002).

35.   C. Koch-Brandt, C. Morgans, Prog Mol Subcell Biol 16, 130-49 (1996).

36.   W. Zhou, L. Janulis, Park, II, C. Lee, Life Sci 72, 11-21 (Nov 22, 2002).

37.   M. Scaltriti et al., Int J Cancer 108, 23-30 (Jan 1, 2004).

38.   S. Bettuzzi et al., Oncogene 21, 4328-34 (Jun 20, 2002).

39.   S. Bettuzzi, Acta Biomed Ateneo Parmense 74, 101-4 (Aug, 2003).

40.   L. Y. Zhang et al., World J Gastroenterol 9, 650-4 (Apr, 2003).

41.   J. A. Menendez, I. Mehmi, D. W. Griggs, R. Lupu, Endocr Relat Cancer 10, 141-52 (Jun, 2003).

42.   M. L. Kireeva et al., Exp Cell Res 233, 63-77 (May 25, 1997).

43.   M. L. Kireeva, F. E. Mo, G. P. Yang, L. F. Lau, Mol Cell Biol 16, 1326-34 (Apr, 1996).

44.   T. M. Grzeszkiewicz, D. J. Kirschling, N. Chen, L. F. Lau, J Biol Chem 276, 21943-50 (Jun 15, 2001).

45.   S. J. Leu, S. C. Lam, L. F. Lau, J Biol Chem 277, 46248-55 (Nov 29, 2002).

46.   S. J. Leu et al., J Biol Chem 278, 33801-8 (Sep 5, 2003).

47.   J. M. Schober, L. F. Lau, T. P. Ugarova, S. C. Lam, J Biol Chem 278, 25808-15 (Jul 11, 2003).

48.   T. M. Grzeszkiewicz, V. Lindner, N. Chen, S. C. Lam, L. F. Lau, Endocrinology 143, 1441-50 (Apr, 2002).

49.   P. F. Choong, A. P. Nadesapillai, Clin Orthop, S46-58 (Oct, 2003).

50.   A. P. Mazar, J. Henkin, R. H. Goldfarb, Angiogenesis 3, 15-32 (1999).

51.   J. B. Smith, H. R. Herschman, Arch Biochem Biophys 330, 290-300 (Jun 15, 1996).

52.   J. B. Smith, H. R. Herschman, J Biol Chem 270, 16756-65 (Jul 14, 1995).

53.   C. G. Lee, J. Demarquoy, M. J. Jackson, W. E. O'Brien, J Immunol 152, 5758-67 (Jun 15, 1994).

54.   M. J. de Veer, H. Sim, J. C. Whisstock, R. J. Devenish, S. J. Ralph, Genomics 54, 267-77 (Dec 1, 1998).

55.   S. F. Altschul et al., Nucleic Acids Res 25, 3389-402 (Sep 1, 1997).